ECSEL Joint Undertaking
Electronic Components and Systems for European Leadership

A European MEMS Ultrasound Benchmark

Scientific White Paper

November 2021

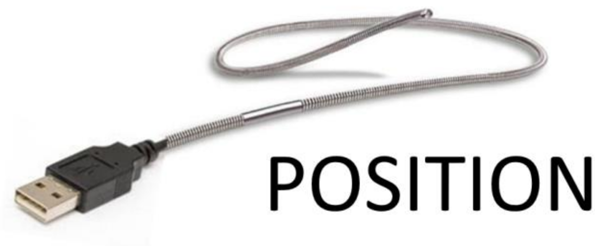

Contact: Nenad Mihajlovic, nenad.mihajlovic@philips.com

Colophon

This White Paper is based on the pan-European MEMS ultrasound transducer benchmark executed in the ECSEL Joint Undertaking project POSITION-2 (grant nr. Ecsel-783132-Position-II-2017-IA).

This White Paper is a publication of the Health.E Lighthouse (https://www.health-lighthouse.eu/). The Health.E Lighthouse is an initiative of the ECSEL Joint Undertaking (https://www.ecsel.eu/lighthouse-initiatives).

The Health.E Lighthouse is supported by the Health.E Lighthouse Support Initiative (HELoS) ECSEL Coordination & Support Action (ECSEL-CSA) grant agreement: 871394

Contact: Nenad Mihajlovic (nenad.mihajlovic@philips.com)

Table of Contents

Table of Contents

1 Executive summary

Europe is at the forefront of the development of the MEMS ultrasound transducers. In this white paper, we summarized the results of a unique Pan-European benchmarking (ref 1) of Micromachined Ultrasonic Transducers (MUTs). The following European companies and institutes with development programs in CMUT and PMUT technology participated in this benchmark: CEA Leti, Fraunhofer Institute for Photonic Microsystems (Fraunhofer IPMS), Imec, Kessler Foundation for Research (FBK), Philips, Roma Tre University, Silex Microsystems AB, Vermon and VTT Technical Research Centre of Finland.

In order to benchmark the MEMS ultrasonic transducers, a set of standard test devices have been defined. Furthermore, common test protocols have been specified and all CMUT and PMUT test structures were characterized using the same air-coupled impedance and acoustic measurement set-ups. Finally, relevant performance parameters have been extracted from the obtained measurement results to provide insights into the available CMUT and PMUT technologies. The benchmark outcome was used to map the different device technologies on the most relevant medical applications, such as echocardiography, gynecology, vascular, intracardiac echocardiography, intravascular ultrasound, ablation, and wearables.

The overall results of the benchmark are:

- There is a difference in the maturity level of CMUT and PMUT technologies. While some partners have more than ten years of experience designing MEMS ultrasonic transducers for various clinical applications, others are doing this for the first time. CMUT technologies are more mature at this moment.
- The most mature conventional and collapse-mode CMUTs showed the best overall acoustical performance and demonstrated comparable round-trip sensitivity. Collapse-mode CMUTs achieve higher transmit pressure, while the best conventional CMUTs have a higher receive sensitivity.
- CMUTs demonstrated a higher bandwidth compared to PMUTs in this benchmark. The higher bandwidth is due to the membrane design freedom that CMUT technologies offer. This is particularly beneficial for high-frequency medical applications.
- PZT-PMUTs show a maximum transmit pressure that is comparable with collapse-mode CMUTs. This high transmit pressure is achieved with a lower radio frequency (RF) driving voltage. Furthermore, this technology demonstrates the best linearity and the lowest harmonic distortion level.
- PMUTs require no (ScAlN and AlN-PMUT) or low operational bias voltage (polymer and PZT-PMUT). Furthermore, at lower RF voltages, PZT-PMUTs achieve a transmit pressure comparable to the best performing collapse-mode CMUTs.

The most mature CMUT technologies are at the level that they can be used in most clinical applications. The main reason for that is due to their maximal pressure, receive sensitivity, and very high bandwidth. High bandwidth CMUTs are interesting since it leads to a high ultrasound imaging resolution. PZT-PMUTs show the potential to be used for therapeutic applications. If this technology is further matured and receive sensitivity is optimized, it has the potential to cover a wider range of diagnostic applications. ScAlN and AlN-PMUTs contain no lead, require no DC bias and are therefore very attractive for medical implant and patch applications. With ScAlN-PMUTs it is possible to achieve higher coupling coefficients than AlN-PMUTs. If both the process and the orientation of the polycrystalline material are further improved, ScAlN may become very attractive for those medical applications. Other PMUT technologies need to be further matured to be used for ultrasound imaging or therapy applications.

Due to their individual characteristics and strength, CMUTs and PMUTs will continue to coexist populating their application areas. Both technologies use semiconductor fabrication technologies and therefore are better suited for miniaturization, integration, and low-cost high-volume production than the state-of-the-art technology based on bulk ceramic piezoelectric materials.

2 Introduction

Today's ultrasonic transducers for medical imaging are dominantly based on poly- or single-crystalline piezoelectric ceramics and composites. These piezoelectric materials became the reference for medical imaging because of their high dielectric constant and high electromechanical coupling coefficient. Piezoelectric ceramics require high-precision mechanical dicing into individual transducer elements making it expensive, especially for the fabrication of 2D arrays for 3D imaging in large consumer-size volumes and manufacture highly miniaturized and high-frequency transducers for use in ICE and IVUS catheters. On the other hand, MUTs can be manufactured using standard microfabrication technologies thus significantly reducing the costly assembly steps needed for conventional piezoelectric and enabling miniaturization and high-frequency broadband operation.

Medical ultrasound uses high-frequency sound pulses to produce images of anatomical structures. Even then, MEMS-based ultrasonic transducers will co-exist with piezoelectric transducers, since all these technologies have their advantages in various clinical and medical applications.

The medical ultrasound application field for ultrasonic transducers is vast. It covers low frequency ultrasound (< 3 MHz) for diagnostics and ablation, medium frequency ultrasound (3-10 MHz) for shallow on-body diagnostics and TEE, and high frequency (>10MHz) for in-body coronary applications such as ICE and IVUS (see Table 1).

Table 1 Examples of ultrasonic transducers used for diagnostic and interventional imaging, and therapy.

Low frequency		Medium frequency			High frequency		
							
Echocardio-graphy	Abdominal	Therapeutic	Gynaecology	TEE	Vascular	ICE	IVUS
1-5 MHz	2-5 MHz	4-8 MHz	5-10 MHz	5-10 MHz	5-15 MHz	5-20 MHz	20-50 MHz

In the context of medical ultrasound applications, MEMS ultrasonic transducers are particularly attractive as they allow for on-body and in-body radiation-free operation together with low production cost, making them potentially appropriate for consumer-size markets. Since the field of MEMS ultrasonic transducers is relatively new and still developing, the most suitable application for each technology cannot yet be identified. Furthermore, there is not even a clear consensus on the best way to characterize these ultrasonic transducers and how to objectively compare the different MUT technologies. In the POSITION-II project, CEA Leti, Fraunhofer IPMS, Imec, Kessler Foundation for Research (FBK), Philips, Roma Tre University, Silex Microsystems AB, Vermon, and VTT Technical Research Centre of Finland, which develop different types of MUTs, collaborated on developing and performing this benchmark.

The approach for the MEMS ultrasonic transducer benchmark consists of four pillars. In the first step, the consortium specified a standard set of test devices with specified aperture, frequencies, elevation length, and element pitch for the test structures. Two different benchmarking specifications were defined, resulting in low frequency and higher frequency test devices. Furthermore, benchmark protocols have been defined that consist of the measurement methods, to obtain the desired quantities, and the analysis methods to translate the measured quantities into general application-related performance characteristics. In the second step, the test structures were manufactured in the different CMUT and PMUT technologies of the project partners according to the test device specifications. In a third step, the common driving electronics, air-coupled impedance, and acoustic measurement set-ups have been completed in order to properly execute the measurements defined in the first step. Furthermore, all available CMUT and PMUT test structures were characterized using the same measurement set-ups under identical circumstances. Finally, the results were evaluated and mapped to the application space. The outcome of the benchmark was used to provide a better understanding of the performance differences of the different MUT technologies in relation to different clinical applications.

3 PMUT/CMUT technologies and manufacturing approaches

3.1 Introduction to MUT technologies

A MUT consists of a thin membrane suspended above a cavity. There are two main types of MUTs, which differ in the transduction mechanism: Capacitive Micromachined Ultrasonic Transducers (CMUT) are based on the electrostatic effect, while Piezoelectric Micromachined Ultrasonic Transducers (PMUT) rely on the piezoelectric effect, see Figure 1 (ref 2).

While traditional piezoelectric transducers are based on the thickness-mode vibration of bulk piezoelectric material or composite, MUT membranes vibrate in flexural mode, resulting in a much lower mechanical impedance. As a result, MUTs are intrinsically better acoustically matched to biological tissue and do not require the use of matching layers typically employed in traditional transducers to achieve broadband operation.

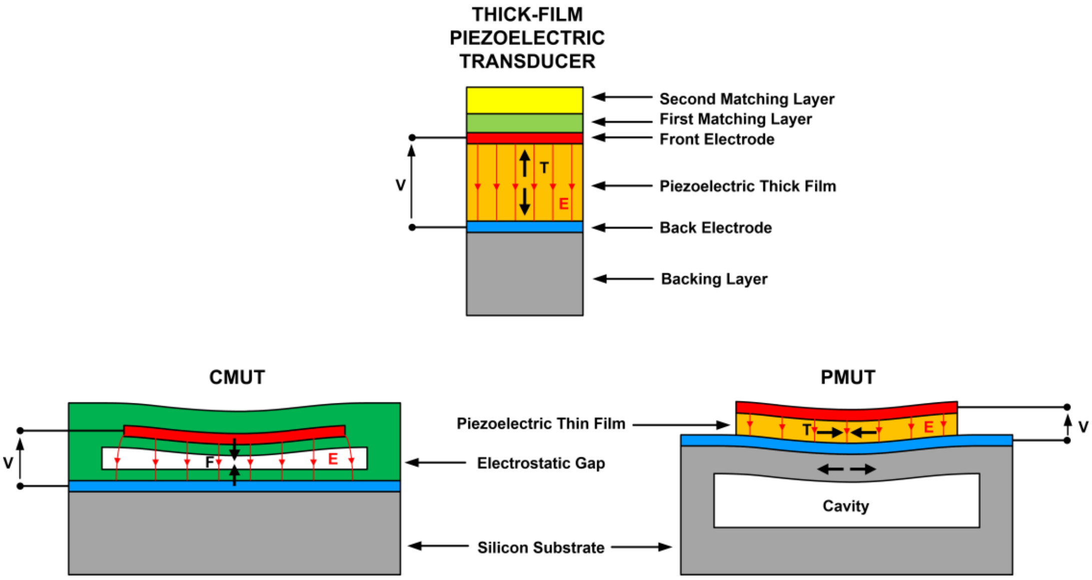

Figure 1 Ultrasound transducer technologies.

3.1.1 CMUT

In a CMUT the vibrating membrane includes a conductive layer, which may be a metallic layer or a doped silicon layer. A conductive substrate acts as the bottom electrode. When a DC voltage is applied over these two electrodes, an electric field is generated inside the cavity, so that the top plate is attracted towards the substrate by an electrostatic force. Driving the CMUT with an AC voltage sets the membrane into vibration and acoustic waves are generated in the surrounding medium. This mechanism also works oppositely. An acoustic wave causing the membrane to vibrate results in a capacitance variation, which is then converted in a variable voltage and/or current under electrical biasing of the CMUT. Efficient and stable electro-mechanical transduction requires generating and maintaining high electric fields in the gap. The key point to generating high acoustic pressures is to maintain large electric fields in the gap. The operating frequency is determined by the dimensions, shape and mechanical properties of the membrane. In collapse mode CMUTs, the cells are designed such that part of the (electrically isolated) membrane is in physical contact with the substrate during normal operation.

3.1.2 PMUT

In a PMUT, the vibrating element consists of a multi-layer structure comprising a piezoelectric thin-film layer metalized on both sides and coupled to an elastic membrane suspended over a cavity. Typically this structure covers part of the membrane. If an AC voltage is applied across the electrodes, an electrical field is generated in the thin-film piezoelectric layer, typically AlN or PZT, which results in stress in the membrane due to the piezoelectric effect. This stress relaxes into a vertical movement of the clamped membrane and thereby generates acoustic waves in the surrounding medium. Vice versa, the piezoelectric effect can also be used to detect acoustic waves impinging on the membrane.

3.2 MEMS ultrasound revolution

Traditional 2D ultrasound images are made using a transducer probe consisting of a row of piezoelectric ceramic (or composite) ultrasound transducers that are organized in a 1D linear array. By pulsing the transducers with a proper phase delay, it is possible to scan an ultrasound beam in one plane resulting in the familiar cross-sectional images. Two developments have stimulated the research into MEMS ultrasound transducers as a replacement for piezoelectric ceramic transducers.

The first development is the trend towards 3D imaging for handheld probes. 3D images require an ultrasound beam that can be steered to scan a volume rather than a plane. For this, a 2D array of ultrasound transducers is needed in which all pixels can be addressed individually with the proper phase delay. State-of-the-art transducers arrays consist of 100 x 100 = 10,000 pixels (ref 3). This poses an enormous interconnection problem. At the moment these 2D arrays are made by solder bumping a slab of piezoelectric ceramic material onto a complex ASIC. After soldering, the individual pixels are separated by dicing. All in all, this is a complex, manual labor-intensive, and thus expensive process. MEMS transducers that can be directly processed on top of the ASIC, or soldered directly on top of the ASIC using TSV technology offer great benefits here.

The second development that has stimulated the development of MEMS ultrasonic transducers is the increasing demand for in-body ultrasound imaging. MEMS transducers have a natural advantage here as they can be much smaller than traditional ceramic transducers while scaling to volume production is straightforward. The flexibility of fabricating MEMS transducer arrays of complex shapes (e.g. circular disks, annular arrays) facilitates the realization of ultrasound imaging catheters that can be placed on the tip of the instrument for forward viewing capability. Additionally, it is relatively easy to scale the devices to higher ultrasound frequencies, see Figure 2 (ref 4). The reason for this is that in conventional ceramic transducers the operating frequency scales with the thickness of the ceramic piezoelectric material: the higher the frequency, the thinner the material. For high frequencies, this results in slabs of material that are too thin to be handled. In MEMS transducers, on the other hand, the operating frequency is simply determined by geometrical dimensions and the thickness of deposited layers.

A comparison of MEMS-based ultrasonic transducers with bulk piezoelectric ceramic transducers is summarized in Table 2.

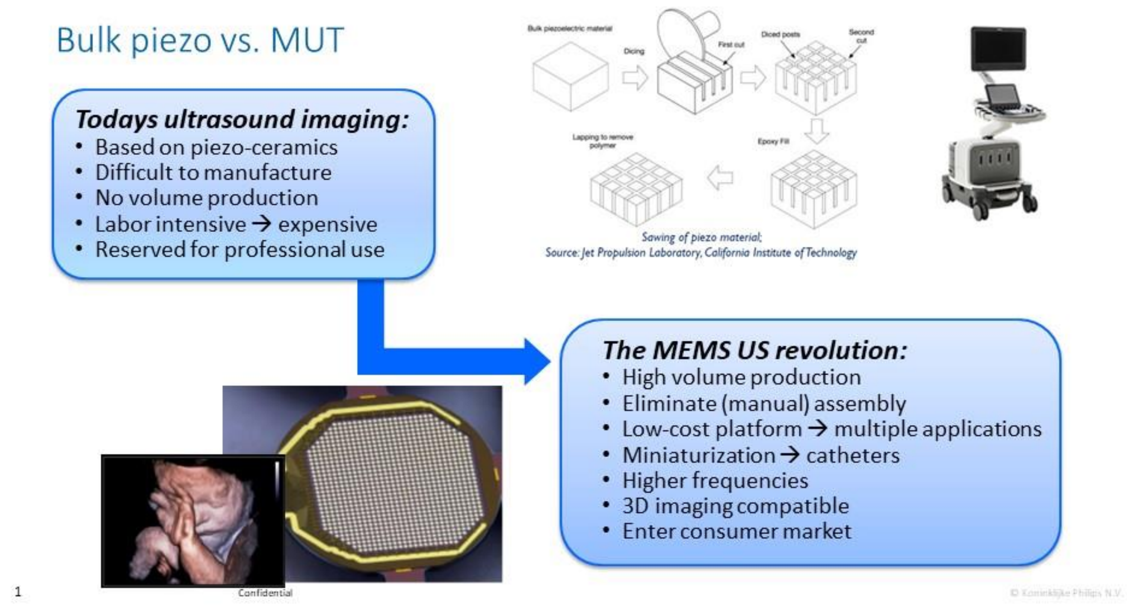

Figure 2 The MEMS ultrasound revolution.

Table 2 Comparison of the characteristics of thick-film piezo transducers, CMUT and PMUT.

	Thick-film piezo transducer	**CMUT/PMUT**
DC bias	Not required	High for CMUT, no or low for PMUT
Frequency range	Typically 1 kHz – 50 MHz	50 kHz – 50 MHz
Electronic integration	Costly, hybrid	Cost-effective, monolithic CMUT on CMOS, flip chip/TSV
Manufacturing	Mechanical dicing	Standard semiconductor processing
Miniaturization	Challenging < 40 µm element size	Element diameter 10 – 400 µm
Design	Limited in element shape. More flexible for curved transducers	Arbitrary element shapes. Advanced techniques needed for curved transducers
Maturity	> 50 y	> 5 y

3.3 Fabrication approaches

Several microfabrication technologies have been developed by various research groups for producing MUT arrays. All MEMS ultrasonic transducers are based on a vibrating membrane. Apart from that commonality, MEMS ultrasonic transducers come in many flavors, each with its advantages and disadvantages (Figure 3). Relating to membrane definition, the two most common approaches for cavity formation are surface micromachining and bulk micromachining. Another division is whether high-temperature process steps are needed. High-temperature steps can be wafer bonding and/or deposition of materials. If monolithic integration is not possible, the MUTs can be manufactured as a separate device that is soldered on top of the ASIC by using advanced interconnection technologies, e.g. 3D packaging and TSV.

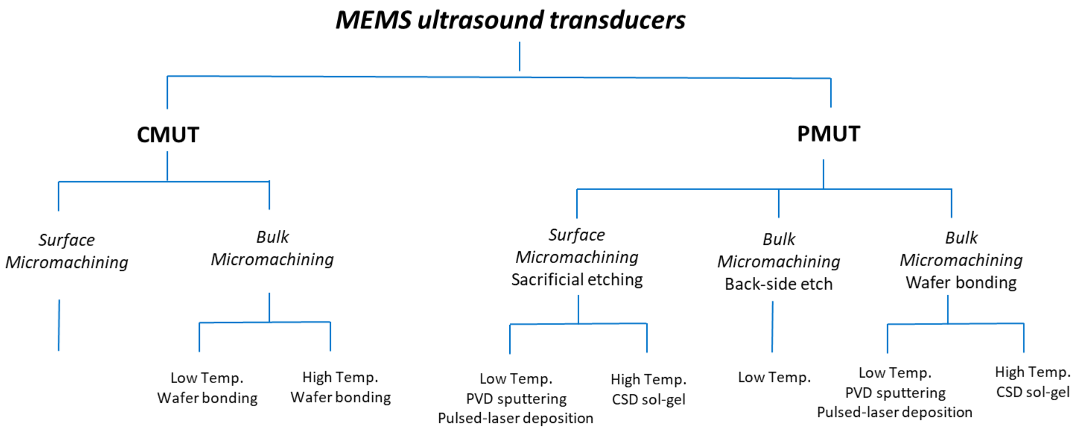

Figure 3 MEMS ultrasonic transducers come in many flavors.

3.3.1 Surface micromachining

In surface micromachining processes, the cavities are defined within a previously deposited layer on top of the substrate, via a sacrificial etch or a photolithographic step. Typical examples of CMUT and PMUT fabrication using the sacrificial method are shown in Figure 4 and Figure 5.

For the CMUT, see Figure 4 (ref 5), starting with depositing a layer of silicon nitride as the insulator on a highly doped silicon wafer and etch-stop-layer followed by a sacrificial polysilicon layer and patterning (a). Next, another layer of polysilicon is deposited to create etch channels for the sacrificial polysilicon etch (b). Afterward, silicon nitride is deposited and patterned. This silicon nitride forms the top plate, and the holes create access to the sacrificial layer (c). The sacrificial polysilicon is removed via the holes with a wet etch (d). The resulting gap is sealed with silicon nitride by low-pressure chemical vapor deposition (e). In the final step, aluminum is deposited and patterned to form the top electrode and electrical contacts (f). The highly doped wafer can be used as the bottom electrode.

For the PMUT, see Figure 5 (ref 6), a silicon layer is doped, and the bottom electrode is deposited (a). Then the access holes are etched in the bottom electrode and the electrode is patterned (b). The next step is the deposition and patterning of the piezo material (c) followed by deposition and patterning of the top electrode (d). The cavity is formed by etching the sacrificial layer via the access holes (e, f).

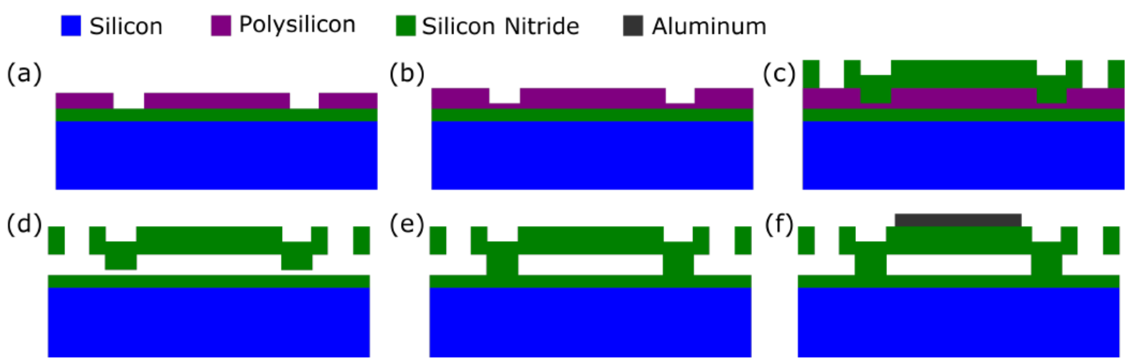

Figure 4 Typical example of a sacrificial release process for CMUT fabrication.

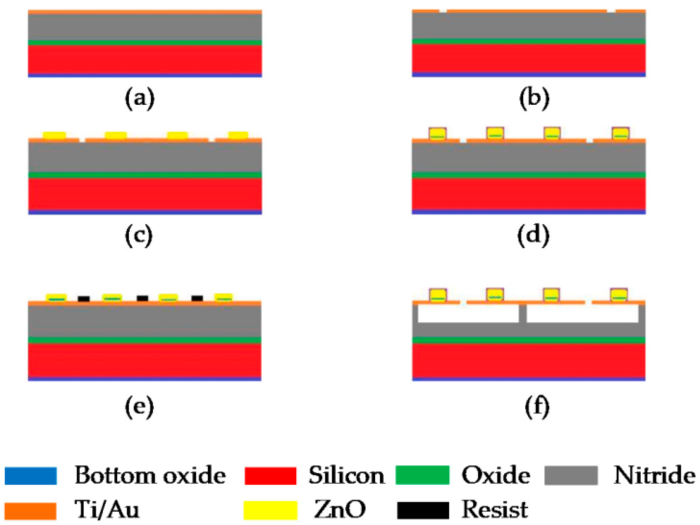

Figure 5 Typical example of a sacrificial release process for PMUT fabrication.

The Polymer-PMUTs utilize surface fabrication compatible with flat-panel display technologies. First cavities are formed by patterning a photoresist on a glass substrate (a). A polyimide membrane is then suspended over the cavities to support the piezoelectric stack (b). The formation of a three-layer stack starts with the deposition and patterning of the bottom electrode (c), followed by the spin coating of a piezoelectric polyvinylidene fluoride P(VDF-TrFE) layer (d), and concluded with the deposition and patterning of the top electrode (e) (ref 7).

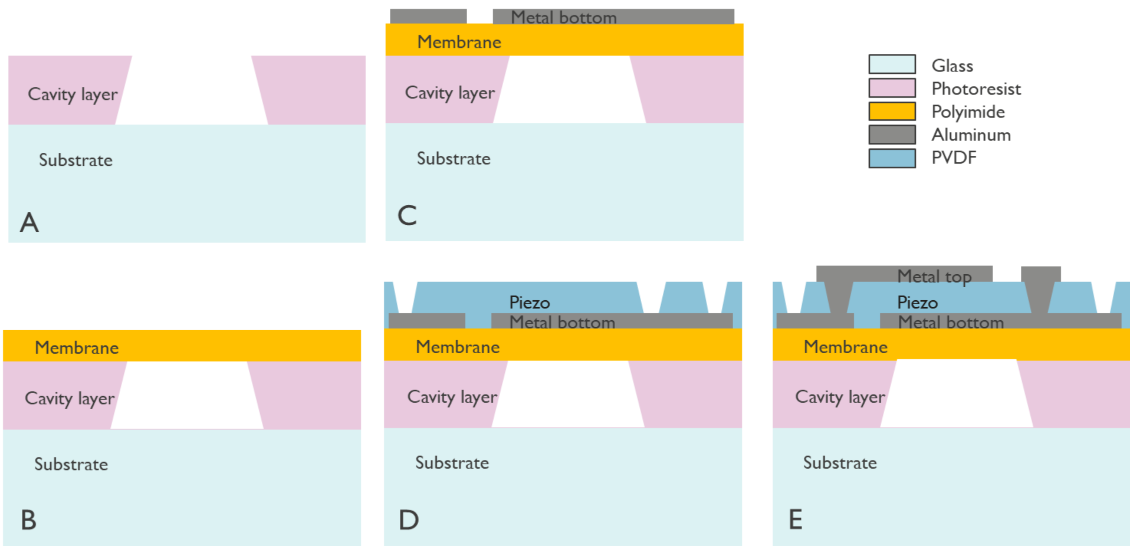

Figure 6 Typical example of a polymer PMUT process flow.

3.3.2 Bulk micromachining

In bulk micromachining processes, the cavities are formed by silicon vertical etching. A common approach to define the membranes in bulk micromachining is to form closed cavities by wafer bonding. In its simplified version, a CMUT wafer bonding process starts with a silicon wafer and a silicon-on-insulator (SOI) wafer (a, b), see Figure 7 (ref 5). The cavity is etched (c) followed by thermal oxidation to grow the insulation layer (d). After an RCA clean (a standard set of wafer cleaning steps) and surface activation, the two wafers are brought together in a vacuum and annealed at high temperature (~1100°C) to form strong covalent bonds (d). The next step is grinding and etching of the handle wafer (e), etching of the buried oxide layer leaving the membrane over the cavities (f) and device isolation (g). Alternatively, one may start with a cavity-SOI wafer. This kind of wafer already features cavities and suspended membranes and may be directly bought from industrial substrate suppliers such as POSITION-II partner Okmetic. This eases the fabrication process at the price of some standardization of the device's properties. In both cases, the process is finalized by removing the buried oxide (g), sputtering metallization (h), patterning the top electrodes (i), and device isolation.

Wafer bonding is also used also for PMUT fabrication, Figure 7 (ref 6). In this case, the piezoelectric stack is formed on top of the membranes of a cavity SOI (C-SOI) wafer.

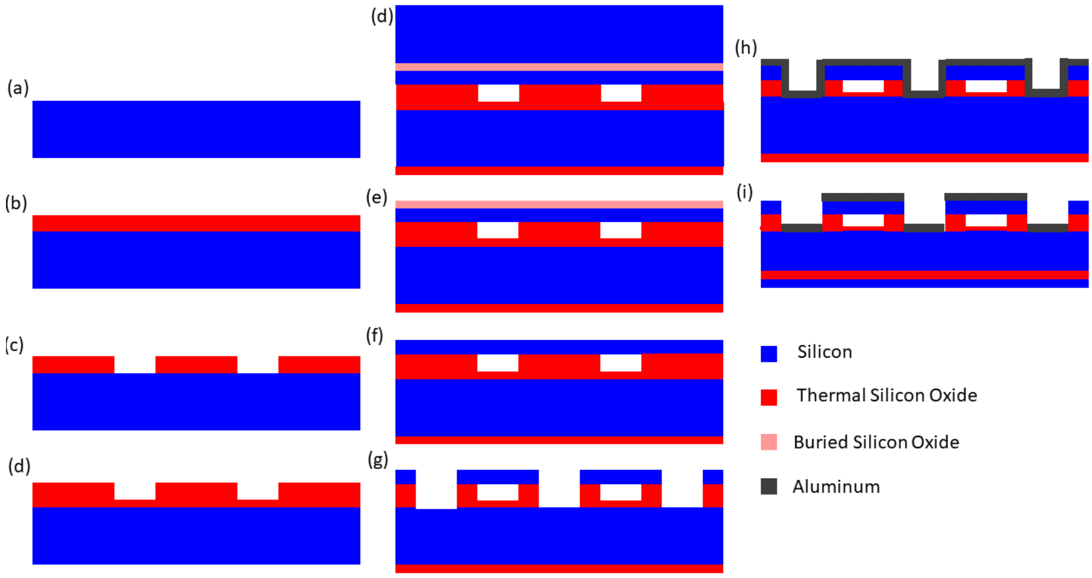

Figure 7 Typical example of a wafer bonding process for CMUT.

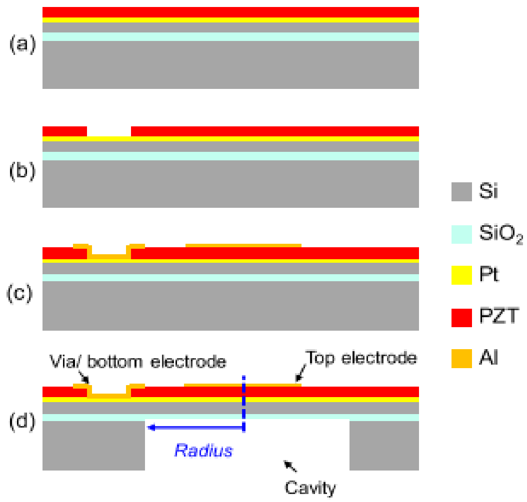

Figure 8 Typical example of cavity formation by back etching of the silicon substrate for PMUT.

3.3.3 MUT devices included in the benchmark

In the POSITION-II project, CEA Leti, Fraunhofer IPMS, Imec, Kessler Foundation for Research (FBK), Philips, Roma Tre University, Silex Microsystems AB, Vermon, and VTT Technical Research Centre of Finland are developing different types of MUTs and more detailed information about that can be found in the appendix. Table 3 below gives an overview of some characteristics of the fabrication approach for the MUT devices included in the benchmark.

Table 3 Overview of the different devices and manufacturing technologies for each partner included in the benchmark.

Partner	MEMS transducer type	Cavity formation	Materials process	CMOS Compa-tibility	Max process temperature (°C)	# masks	Starting wafer type	Wafer size (mm)
CEA-Leti Technology Research Institute	CMUT AlN-PMUT	Wafer bonding Wafer bonding	Si membrane Sputtered AlN	Yes	 400	6 6	Si low resistivit y and SOI Si and SOI	200
Fraunhofer Institute For Photonic Microsystems	CMUT	Sacrificial release	Sputtered TiAl	Yes	400	8	Si	200
Imec	Polymer-PMUT	Cavity etch, membrane bonding.	Polymer membrane, spin coat PVDF.	No	350	4	Glass	150
Philips	Collapsed-CMUT	Sacrificial release	SiN membrane	Yes	400	6	Si	200
Roma Tre University/FBK	CMUT	Sacrificial release	SiN membrane	Yes	300	7	Si	150
Silex Microsystems	PZT-PMUT		Sputtered PZT	Yes. PZT after FEOL	500	5	SOI or CSOI	200
Vermon	AlN-PMUT	Sacrificial release	Sputtered AlN	Yes	400	9	Si	200
VTT	AlN-PMUT ScAlN-PMUT		Sputtered AlN/ScAlN	Yes	400	4	CSOI	150

4 Benchmark approach

4.1 Introduction

The main objective of this benchmark is to come to a better understanding of the advantages and disadvantages of the different MEMS ultrasonic transducer concepts, both from a technology as well as from an application point of view. To achieve this objective, eight of the foremost institutes and companies working in this field in Europe have agreed to participate in a pan-European technology benchmark (Figure 9). The fact that a number of the participants are direct commercial competitors emphasizes the importance of such a benchmark.

The MUT devices developed in POSITION-II should have similar specifications in order to provide comparable and fair conditions for the benchmark. The common benchmark specifications also made sure that all the fabricated devices were compatible with the common test protocol and the test setup for benchmarking.

After optimizing the drive conditions such as bias voltage and RF voltage, the following measurements were performed:

- air-coupled impedance measurements
- acoustic measurements in water

Figure 9 Participants in the pan European MEMS ultrasonic transducer benchmark.

4.2 Test set-ups and protocols

4.2.1 Test devices

Considering the very broad range of applications that may be addressed by the CMUT and PMUT technologies, it has been agreed to focus only on the 1-10 MHz frequency range to avoid unmanageable complexity and to ease the measurements. However, 1-10 MHz is still quite a large frequency range and covers several different applications requiring different key performances and technological compromises. Furthermore, electrical and acoustical performances are very dependent on the operating frequency. Finally, the level of performance and maturity can vary from partner-to-partner and technology-to-technology across this frequency range.

Therefore, it has been agreed to produce two types of devices for benchmarking: low frequency (LF) and high frequency (HF) devices. The device specifications are given in Table 4. In Figure 10, a sketch of a test device is shown. Each partner has been free to select which types of devices they wanted to manufacture.

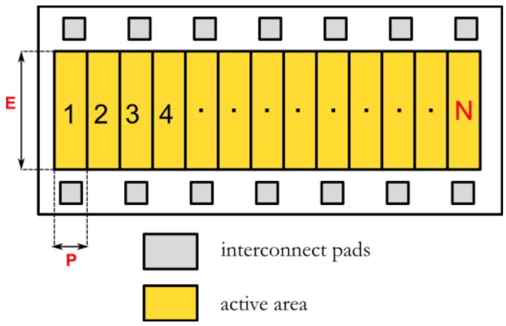

Figure 10 Scheme of the MUT test devices

Table 4 Parameters defining LF and HF MUT test devices.

Parameter	LF	HF
Center frequency f_c [MHz]	2.4 - 3.2	8
Pitch P [µm]	225 - 315	200
Elevation E [mm]	12 - 14	5
Number of elements N [1]	6 - 80	96

4.2.2 Air-coupled impedance measurements

The measurement of the electrical impedance of a transducer is carried out on a wafer level with automatic probing stations. It is performed on single CMUT and PMUT lines using Keysight Impedance Analyzer E4990A 20Hz-120MHz (see Figure 11). Furthermore, a biasing circuit unit is applied.

The measured electrical impedance Z is fitted using a simplified lumped element resonator model shown in Figure 12 and the following information is extracted from the impedance measurement results (ref 8):

- capacitances at low C_{LF} and high frequencies C_{HF} [pF]
- electrical resonant f_r and anti-resonant frequencies f_a of the MUT diaphragms [MHz]
- the series resistance R_s [Ω]
- the parallel capacitance C_p [pF]
- the mechanical capacitance C_m [pF]
- electromechanical coupling coefficient k_t^2

An example of the curve fitted to the measured electrical impedance Z can be seen in Figure 13.

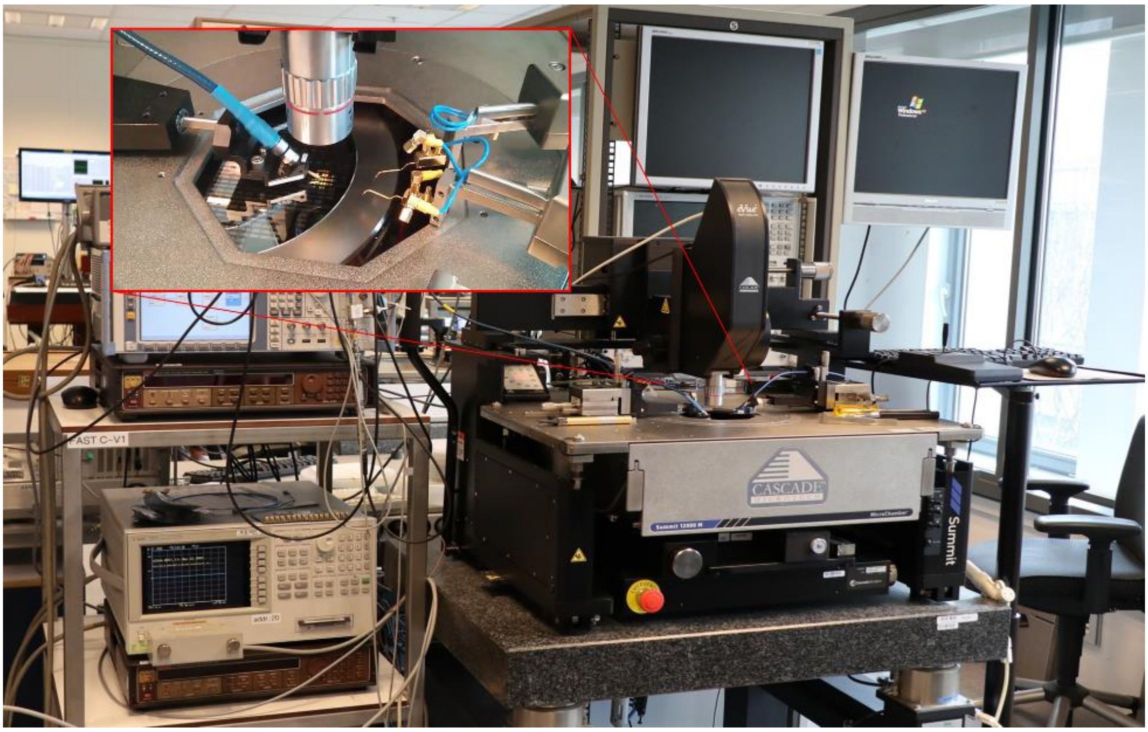

Figure 11 Set-up for air-coupled impedance measurements.

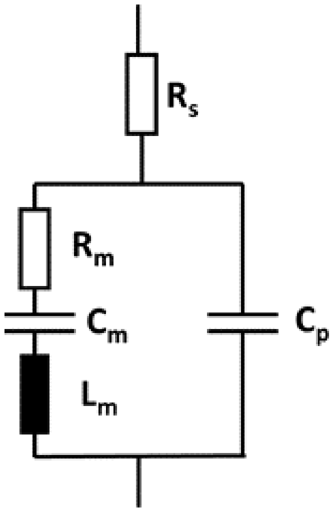

Figure 12 Lumped element model representing a PMUT / CMUT device.

Capacitances at low and high frequencies

Capacitances at low and high frequencies (C_{LF} and C_{HF} respectively) are determined at the lowest (100kHz) and highest (40MHz) frequencies of the frequency range set on the impedance analyzer, respectively.

Electrical resonant and anti-resonant frequencies

Electrical resonant (f_r) and anti-resonant (f_a) frequencies define the minimum of the magnitude of the electrical impedance and admittance, respectively (ref 9).

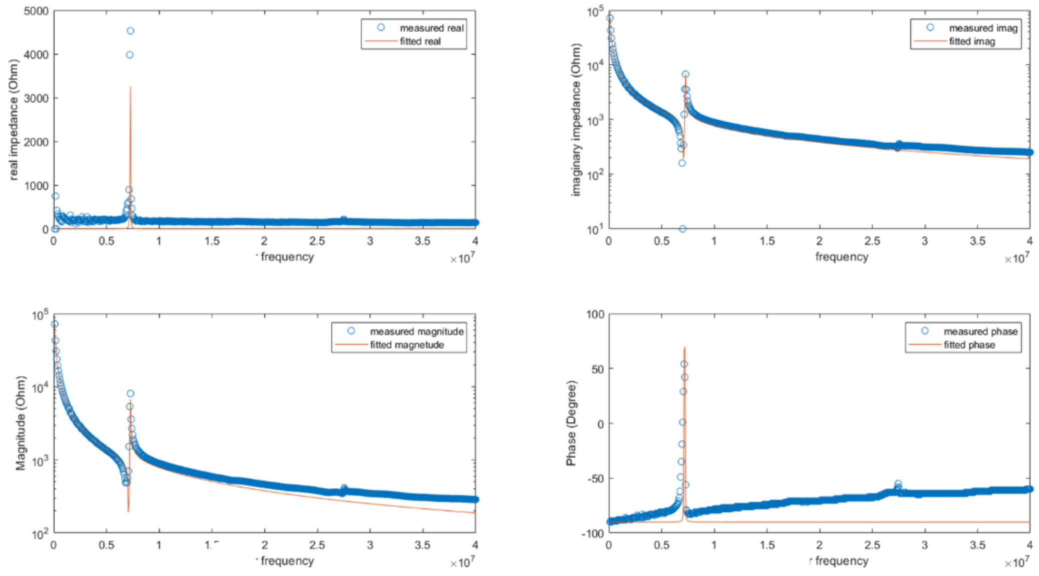

Figure 13 An example of impedance measurement and the fitted curve.

Series resistance

Series resistance R_s is determined at the highest measured frequency (40MHz) of the impedance measurement. It is evaluated in a constant region of the real part of the impedance.

Parallel capacitance

Parallel capacitance C_p is equal to the measured C_{HF}.

Equivalent electromechanical parameters

The equivalent electromechanical parameters represent the PMUT/CMUT device at resonance as an electrical equivalent circuit. The equivalent mechanical capacitance $C_m = C_{LF} - C_p$ represents the device mechanical compliance and transduction mechanism as an electrical capacitor. The equivalent mechanical inductance L_m represents the device's effective mass. The equivalent series resistance R_m represents the motional losses at resonance.

Electromechanical coupling coefficient

Electromechanical coupling coefficient k_t^2 describes the efficiency of the transduction. It is defined as the ratio between the mechanical energy and the total energy of the device. It can be obtained from the electrical resonant and anti-resonant frequencies, or the low frequency and high-frequency capacitances (ref 10):

$$k_t^2 = 1 - \frac{f_r^2}{f_a^2} = 1 - \frac{C_{HF}}{C_{LF}} \quad (1)$$

4.2.3 Acoustic measurements

All acoustic measurements were performed using dedicated transmit-receive driving electronics with a PCB on which the CMUTs and PMUTs devices are mounted (Figure 14). The dies under test were wire-bonded so that multiple MUT lines were connected in parallel. All dies received the same acoustic window made from about 20 µm PDMS and 5 µm Parylene C. For the Polymer-PMUTs, the chosen acoustic window has been comparable in thickness and stiffness to the device membrane. Therefore only 700 nm of Parylene C was used to enable measurements on these devices.

The acoustic transmit and pulse-echo test set-ups are shown in Figure 15-15. The test protocols and the extraction of relevant performance parameters are performed according to what has been described in related standards (ref 11 and ref 12). For example, a transducer and hydrophone positioning system is used whose hydrophone alignment procedures follow the description in ref 11. Furthermore, a calibrated PVDF membrane hydrophone (ref 13) is applied, the type of which is in the recommended hydrophone list in ref 10. The hydrophone has been calibrated up to 30 MHz. The oscilloscope output impedance is well matched with the cable impedance.

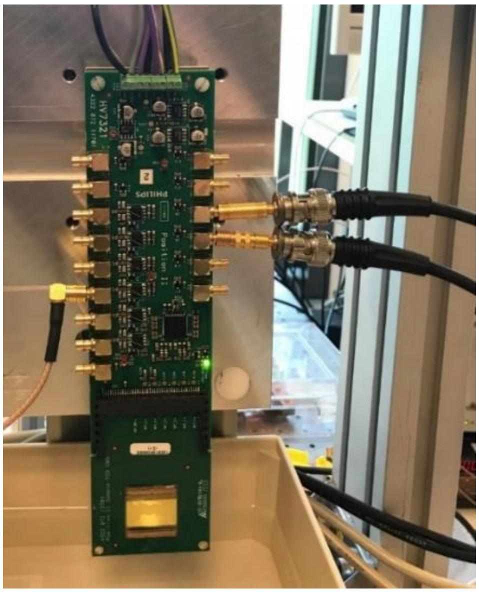

a)

b)

Figure 14 a) Transmit-receive driving electronics board with PCB on which device under test is mounted, b) PCB with a device under test.

Figure 15 The set-up used for acoustic measurements (overview).

In this benchmark study, statistics over the performance were not determined due to a limited number of accessible samples. Instead, the focus of the measurements was to properly optimize the test set-ups and collect measurements of all the available technologies from each of the partners. Despite the various limitations, partners involved found that the results presented in this report represent very well the status of the device that has been characterized.

The acoustic transmit measurements were done in the near-field (NF) as close as possible to the surface of the device under test and at a far-field (FF) distance. The set-up that is used for the transmit measurements is shown in Figure 16. We selected the following protocols as most important for the acoustic transmit measurements:

1.) Impulse response: a unipolar single 20 ns pulse at NF and FF. The pulse is always additive to the applied DC voltage if a DC bias is applied.

2.) Linearity measurement: 2-cycles bipolar at the center frequency f_c (see next page) of the device. The RF voltage is increased step by step to the maximally allowed peak-peak voltage. Measurement is done at NF and FF.

3.) Harmonic measurement: 10-cycles bipolar at 2/3 of the center frequency f_c. The RF voltage is increased step by step to the maximal allowed peak-peak voltage. The purpose of this measurement is to investigate the 2nd harmonic content at 2 * 2/3 f_c as a function of transmit pressure. This indicates whether the device under test is useful for 2nd harmonic imaging modality. This measurement is done in the NF (surface) only.

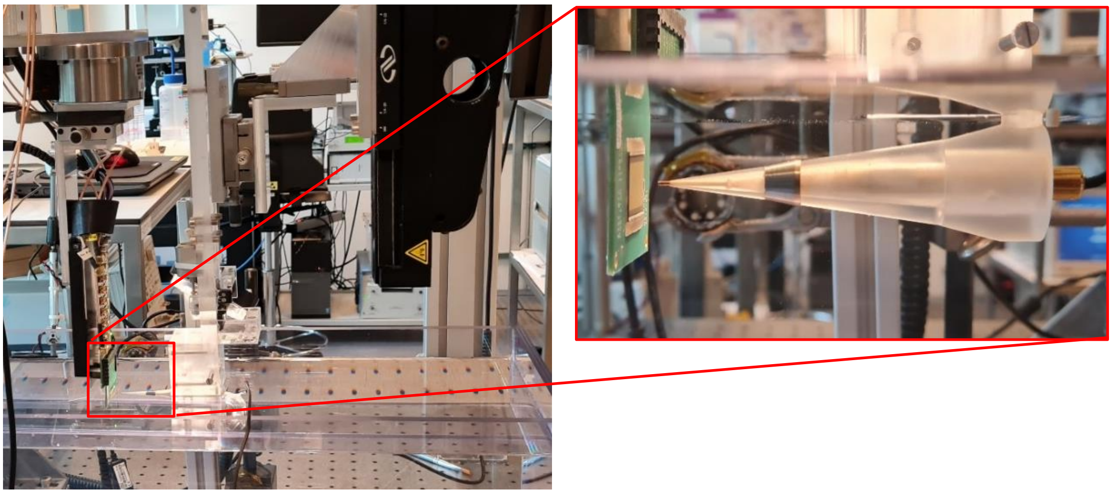

a) b)

Figure 16 Set-up used for acoustic transmit measurements. In a) positioning systems for driving electronic board and for hydrophone are seen and in b) a hydrophone can be seen when positioned for CMUT/PMUT characterization.

For pulse-echo measurements were performed only at FF using a stainless-steel metal plate as an acoustic reflector. The set-up used for those measurements is shown in Figure 17. The following protocols were selected for the pulse-echo measurements:

4.) Impulse response: the unipolar single pulse of 20 ns width (setting 25 MHz) at FF.

5.) Linearity measurement: 2-cycles bipolar at the center frequency f_c of the device. The RF voltage is increased step by step to the maximal allowed peak-peak voltage. Measurement is done at FF.

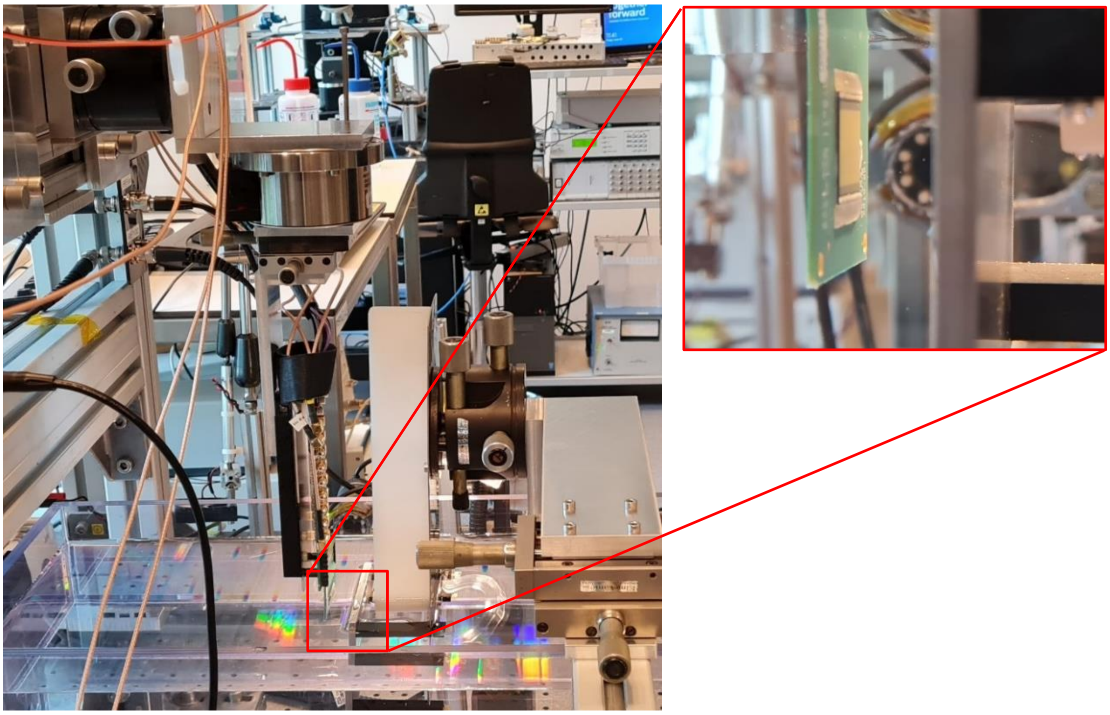

a) b)

Figure 17 Set-up used for pulse-echo measurements. In a) positioning systems for metal reflector can be seen and in b) a metal reflector can be seen when positioned for CMUT/PMUT characterization.

In all measurement protocols used for testing the CMUTs and PZT PMUTs, the optimal bias, RF driving voltage, and frequency were used for each CMUT and PMUT device. Optimal driving conditions (DC bias, RF voltage and driving frequency) are defined iteratively in order to obtain the highest transmit pressure and roundtrip sensitivity without degrading or damaging the device under test.

The following information is extracted from those measurements:

- DC bias voltage V_{BIAS} [V]
- RF peak-to-peak voltage V_{PP} [V]
- maximum peak-to-peak acoustic pressures P_{max} [Pa]
- transmit sensitivity T_x [Pa/V]
- center frequency f_c [MHz]
- absolute bandwidth BW [MHz]
- fractional bandwidth BW% [%]
- harmonic distortion HD [dB]
- roundtrip sensitivity TR_x
- receive sensitivity R_x [V/MPa]

DC bias voltage

The DC bias voltage V_{BIAS} is determined experimentally when defining the optimal driving condition of each CMUT and PMUT device.

RF peak-to-peak voltage

The RF peak-to-peak voltage V_{PP} is extracted from the measured time-domain RF voltage that is recorded during acoustic measurements. The maximum allowed RF voltage represents a maximal voltage of the device that can be applied for the optimal DC bias voltage without destroying or degrading the device.

Maximum peak-to-peak acoustic pressure

The maximum peak-to-peak pressure P_{max} is extracted from the time-domain acoustic pressure signal that is recorded from the hydrophone measurements. The linearity transmit measurement in NF is used.

Transmit sensitivity

The transmit sensitivity T_x is determined from the slope of the linearity curve (pressure versus RF voltage) for small RF voltages.

Center frequency

The center frequency f_c is defined as the arithmetic mean between the low and high frequencies at 3dB down from the spectral maximum of the recorded time-domain acoustic pressure signal. Impulse response transmit measurement protocol is used in FF.

Absolute bandwidth

The absolute bandwidth BW is the range bounded by the low and high frequencies at 3dB down from the spectral maximum of the recorded time-domain acoustic pressure signal. Impulse response transmit measurement protocol is used in FF.

Fractional bandwidth

The fractional bandwidth BW% is the ratio between absolute bandwidth BW and center frequency f_c expressed in percentage.

Harmonic distortion

The harmonic distortion HD is assessed for the 2^{nd} harmonic component only, with regards to the fundamental frequency. It is defined as the level of the 2^{nd} harmonic amplitude with regard to the fundamental frequency of the spectrum. It is obtained using harmonic measurement protocol.

Roundtrip sensitivity

The roundtrip sensitivity TR_x is calculated from the received echo signal per applied RF voltage in a pulse-echo measurement.

Receive sensitivity

The receive sensitivity R_x is the round trip sensitivity divided by the gain of the receive amplifier. The impulse response pulse-echo protocol is used. The result is then divided by the transmit sensitivity measured with the hydrophone at the same measurement distance.

5 Benchmark results

5.1 Technology results

This chapter reports the results of the benchmark for the different MUT technologies. For each MUT technology, the results for the low frequency (approx. 3 MHz) and high frequency (approx. 8 MHz) devices are reported.

5.1.1 Bias voltages

The CMUT devices typically need a DC bias voltage of 70-160V. PZT-based PMUT devices and polymer-based PMUT devices need a small DC bias (< 50V) and AlN-based PMUT devices need no DC Bias voltage. The picture below shows the voltages applied during the benchmark.

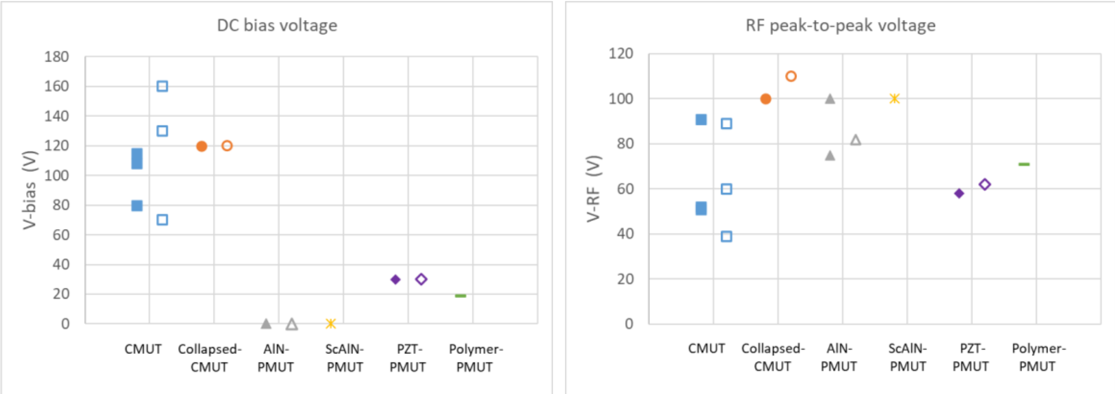

Figure 18 Operating voltages used during the benchmarking: DC bias voltage (left) and RF peak-to-peak voltage (right). For each MUT technology, the LF devices are marked with filled markers (e.g. ●) and the HF devices are marked with open markers (e.g. **o***). ScAlN and polymer PMUT have only LF device variant.*

5.1.2 Air-coupled impedance measurement results

The electromagnetic (EM) coupling coefficient is an important parameter that gives the ratio of mechanical energy to the total stored energy. The EM coupling coefficient depends on the design (e.g. frequency) and the bias voltage (for CMUT) and is considered a good indicator for the device quality, efficiency and performance (peak pressure, transmit sensitivity, receive sensitivity).

Figure 19 below gives an overview of the EM coupling coefficient for all benchmark devices. The large variation for conventional CMUT devices shows the differences in maturity between the partners. The highest values are reached for the most mature conventional and collapsed CMUT devices.

PZT-PMUT devices are able to achieve a moderate EM coupling coefficient. Note that there were experimental difficulties in determining the coupling coefficient for the HF PZT-PMUT devices, and consequently the accuracy of the reported values is limited.

The benefit of doped ScAlN over non-doped AlN is already visible. The other PMUT technologies need to be further matured.

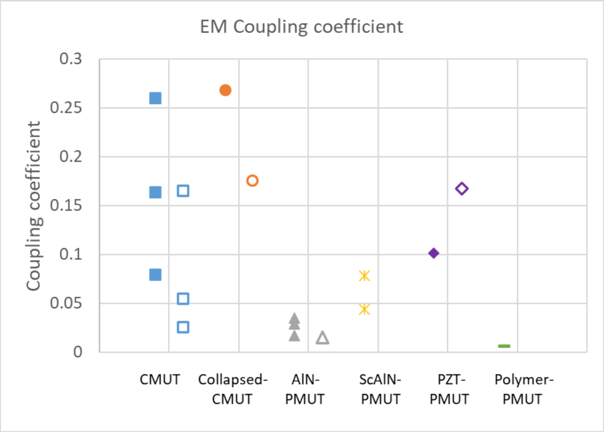

Figure 19 EM coupling coefficient (k_t^2) for all benchmark devices. For each MUT technology, the LF devices are marked with filled markers (e.g. •) and the HF devices are marked with open markers (e.g. **o***). ScAlN and polymer PMUT have only LF device variant.*

Figure 20 and Figure 21 give the parallel capacitance, equivalent mechanical capacitance and series resistance of the benchmark devices. A low value for the series resistance is generally preferred to minimize power consumption and heat generation. Low series resistance is especially important for high capacitance devices that are more demanding for the driver electronics in terms of current. A high series resistance relates to the maturity of the technology and needs further optimization.

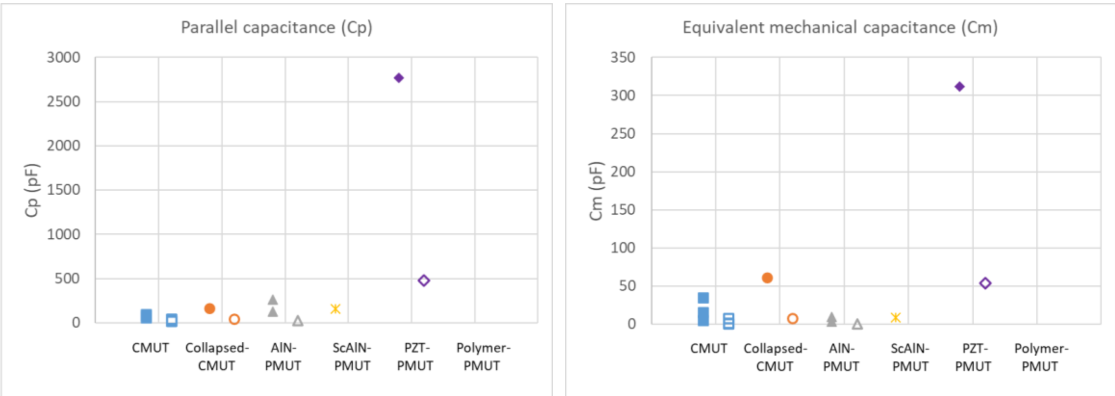

Figure 20 Parallel capacitance (left) and equivalent mechanical capacitance (right). For each MUT technology, the LF devices are marked with filled markers (e.g. •) and the HF devices are marked with open markers (e.g. **o***). ScAlN and polymer PMUT have only LF device variant.*

From the basic equivalent circuit of a MUT (Equation 1), since $C_{HF} = C_p$ and $C_{LF} = C_m + C_p$, the following is obtained

$$k_t^2 = \frac{C_m/C_p}{1+C_m/C_p}. \qquad (2)$$

Figure 22 confirms that data extraction from the impedance measurements has been done consistently. All devices follow a line described by Equation 2 except the HF PZT-PMUT device. The latter originates from experimental difficulties in determining the EM coupling coefficient.

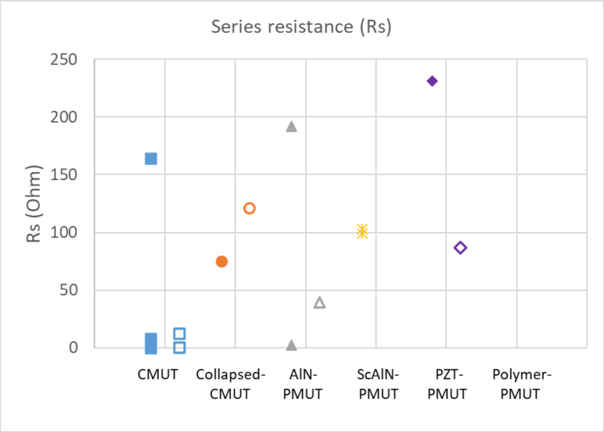

*Figure 21 Series resistance. For each MUT technology, the LF devices are marked with filled markers (e.g. ●) and the HF devices are marked with open markers (e.g. **o**). ScAlN and polymer PMUT have only LF device variant.*

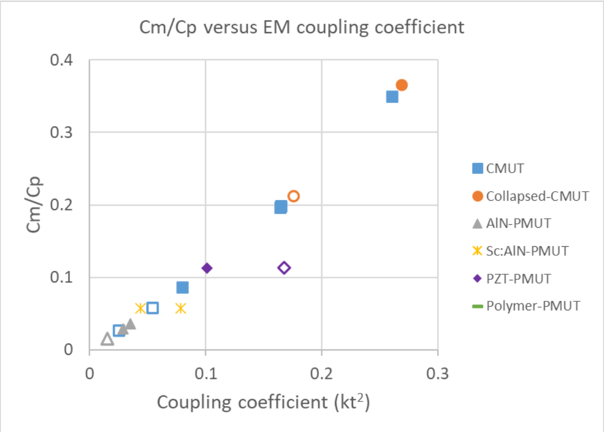

*Figure 22 Relation between C_m/C_p and the coupling coefficient. Note that the accuracy of the coupling coefficient for PZT-PMUT devices is limited. For each MUT technology, the LF devices are marked with filled markers (e.g. ●) and the HF devices are marked with open markers (e.g. **o**). ScAlN and polymer PMUT have only LF device variant.*

5.1.3 Acoustic performance

Bandwidth

The bandwidth (BW) is generally related to both the geometry (thickness and area) and the material parameters (Young's modulus, density, and Poisson's ratio) of the membranes, as well as to the fill factor (ratio of the membrane's area to the total area).

While broadband operation at low frequencies can be obtained with most technologies, broadband operation at high frequency is more challenging to achieve, as smaller and thinner membranes (ref 14) and high fill factors, are required (ref 15), and not all technologies have the same freedom to reduce the membrane thickness and the cell-to-cell distance.

An overview of the fractional BW for the benchmark devices is shown in Figure 23. There is a clear difference between LF and HF devices, where we see a smaller BW for the HF devices.

Figure 24 gives the fractional BW versus center frequency. This graph visualizes the generic decrease of BW with frequency. The large variations of fractional bandwidth are not only technology and maturity related, but also the result of different design choices that were made for the current benchmark.

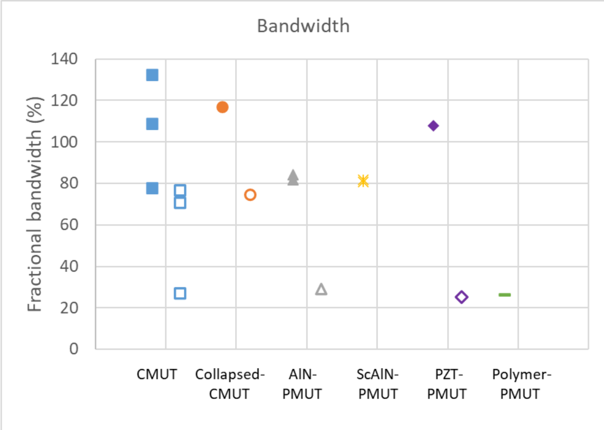

Figure 23 Fractional bandwidth (-3dB) from far-field impulse response. For each MUT technology, the LF devices are marked with filled markers (e.g. ●) and the HF devices are marked with open markers (e.g. o). ScAlN and polymer PMUT have only LF device variant.

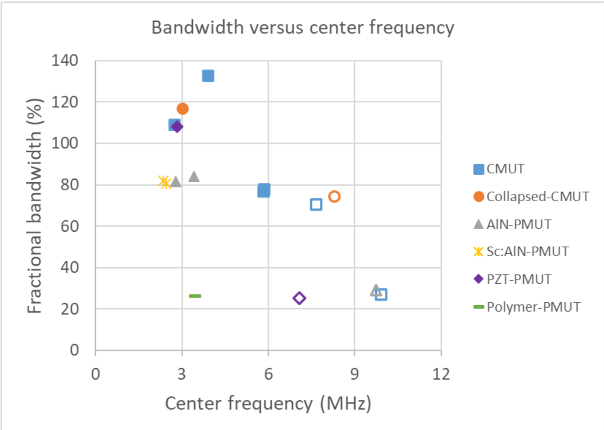

Figure 24 Fractional bandwidth (-3 dB) versus center frequency. For each MUT technology, the LF devices are marked with filled markers (e.g. ●) and the HF devices are marked with open markers (e.g. o). ScAlN and polymer PMUT have only LF device variant.

In general, CMUT devices can have a larger BW than PMUTs at higher frequencies as a result of the increased membrane design freedom. In CMUTs, the membrane thickness can be made smaller in CMUTs than in PMUTs, resulting in a lower mechanical impedance and hence a lower Q factor vibration and acoustic radiation in immersion operation.

Maximum peak-to-peak pressure

The maximum peak-to-peak pressure not only depends on the technology. This parameter is also determined by the device design, drive conditions and the quality of the device. In the benchmark, the devices were operated at conservative conditions. This was done because the ultimate driving conditions (close to breakdown) were unknown (dedicated device design, low volume, first wafer), and the devices should survive all test protocols.

Figure 25 shows the peak-to-peak pressures for the benchmark devices. CMUTs show high peak pressures where the highest peak pressures are obtained with collapsed-CMUTs devices. The large variation is caused by differences in maturity levels between the partners, where the most mature technologies give the best values. PZT-PMUTs show peak-to-peak pressures comparable to collapsed-CMUTs. Despite the limited maturity of AlN-based PMUTs, the beneficial effect of Sc-doped AlN is already visible.

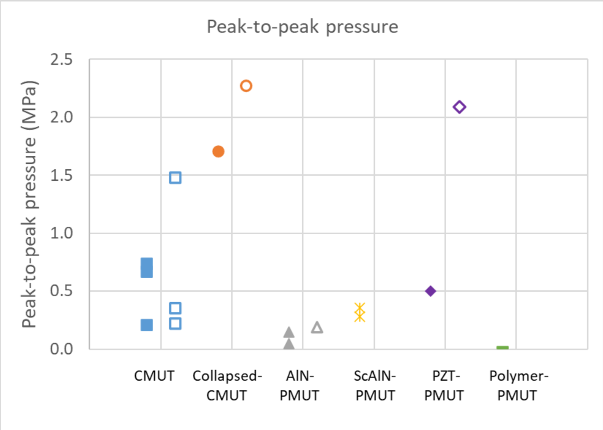

Figure 25 Peak-to-peak pressures (near-field). For each MUT technology, the LF devices are marked with filled markers (e.g. •) and the HF devices are marked with open markers (e.g. **o***). ScAlN and polymer PMUT have only LF device variant.*

Transmit, receive and roundtrip sensitivity

The transmit sensitivity is the increase in peak-to-peak pressure per unit RF peak-to-peak voltage. An overview of the transmit sensitivities for the benchmark devices is shown in Figure 26. This overview is very similar to the overview with the peak-to-peak pressures in Figure 25, except that the PZT-PMUT device here shows the best results.

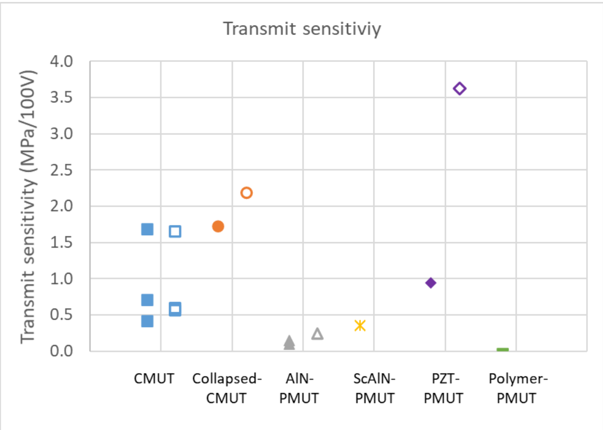

Figure 26 Transmit sensitivity (near-field). For each MUT technology, the LF devices are marked with filled markers (e.g. •) and the HF devices are marked with open markers (e.g. **o***). ScAlN and polymer PMUT have only LF device variant.*

Figure 27 shows the receive sensitivities. The highest receive sensitivity is obtained with the most mature CMUT technologies. This graph also shows that the receive sensitivity of HF devices is lower than the receive sensitivity of LF devices.

The higher sensitivity for the AlN-PMUT compared to PZT-PMUT devices can be understood from the lower dielectric constant of AlN (approx. 100x lower than PZT). For PZT-PMUTs the low receive sensitivity is related to the high capacitance.

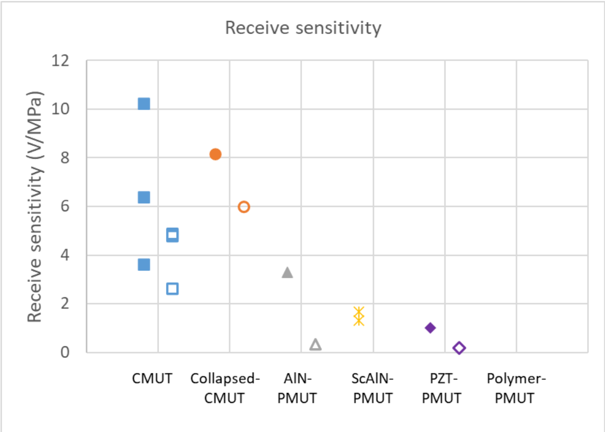

*Figure 27 Pulse-echo receive sensitivity. For each MUT technology, the LF devices are marked with filled markers (e.g. ●) and the HF devices are marked with open markers (e.g. **o**). ScAlN and polymer PMUT have only LF device variant.*

Figure 28 shows the relation between receive and transmit sensitivity and EM coupling coefficient. Overall, a high EM coupling coefficient seems to be a good indicator for the device quality and a high receive and transmit sensitivity.

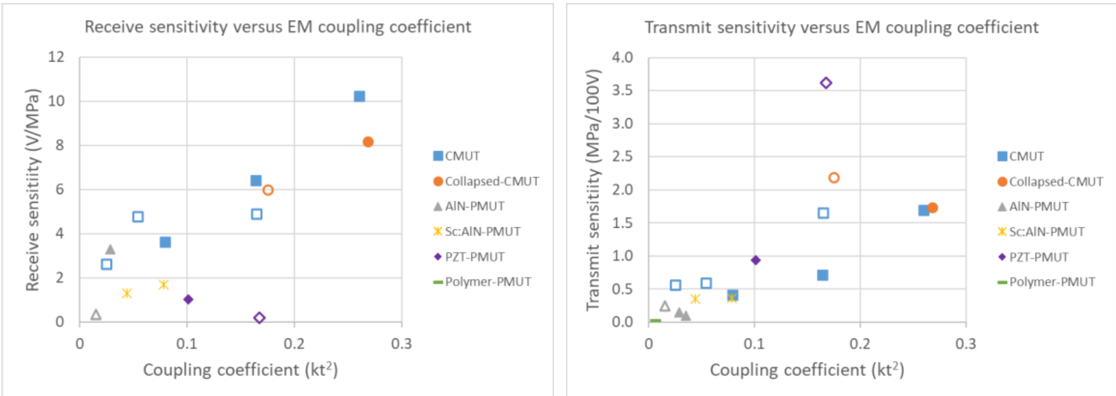

*Figure 28 Receive sensitivity (left) and transmit sensitivity (right) versus EM coupling coefficient. For each MUT technology, the LF devices are marked with filled markers (e.g. ●) and the HF devices are marked with open markers (e.g. **o**). ScAlN and polymer PMUT have only LF device variant.*

For medical imaging, both the transmit and the receive sensitivity are of importance. This combination is represented in the so-called roundtrip sensitivity, which is the product of transmit and receive sensitivity. Figure 29 shows the roundtrip sensitivity values for the benchmark devices, as well as a plot with receive versus transmit sensitivity. Also in this plot, the most mature CMUT technologies give the best roundtrip sensitivity.

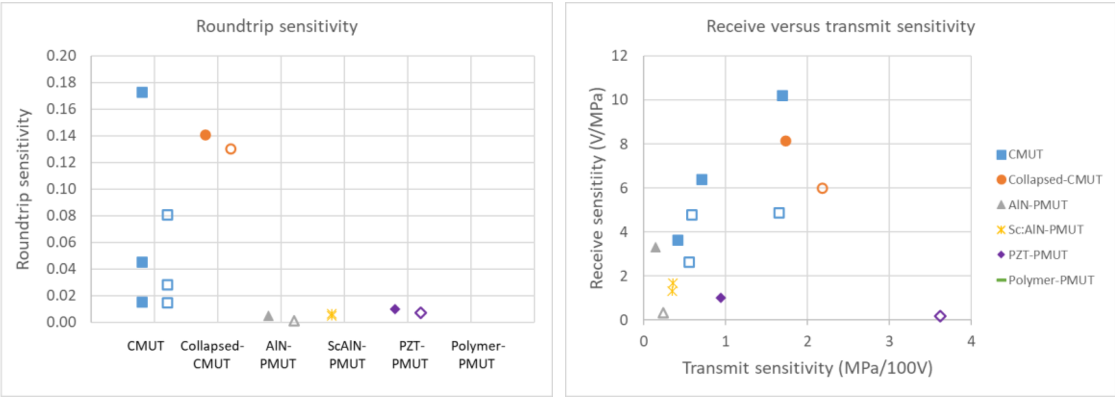

*Figure 29 Roundtrip sensitivity (left) and receive versus transmit sensitivity (right). For each MUT technology, the LF devices are marked with filled markers (e.g. •) and the HF devices are marked with open markers (e.g. **o**). ScAlN and polymer PMUT have only LF device variant.*

Linearity and second harmonic content

Figure 30 shows the relationship between the near-field peak-to-peak pressure and the RF drive voltage.

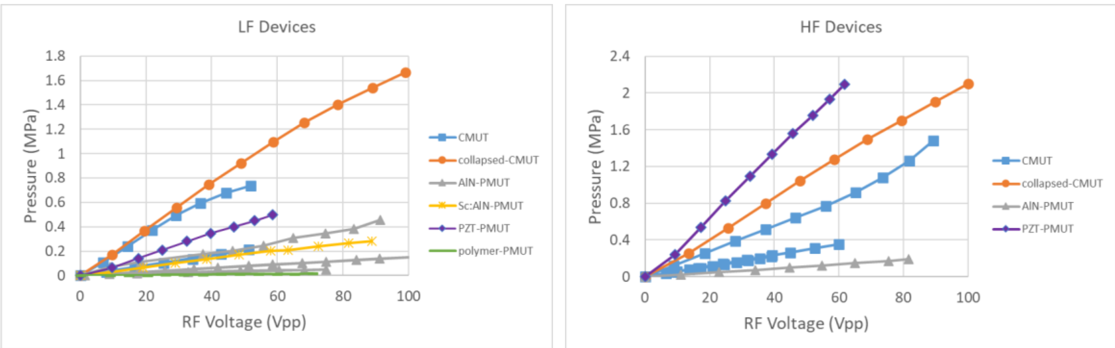

Figure 30 Pressure versus RF voltage, showing device linearity of LF devices (left) and HF devices (right). The lines are only a guide for the eye.

PZT-PMUT and some of the CMUT devices show very good linearity. Note that the varying linearity results for AlN-based PMUTs may be due to the low pressure levels and the resulting limited measurement accuracy of these pressures.

The different devices are also compared in terms of their capability to support 2nd harmonic imaging. In this modality, the transducer emits an ultrasound pulse within the fundamental band. In receive the 2nd harmonic of the signal is measured. For a given device, the 2nd harmonic content is not constant and increases with driving voltage and output pressure. Therefore in Figure 31 the 2nd harmonic content at the same output pressure of 0.7 MPa is compared. Benchmark devices that were not able to reach this pressure level were not included.

The 2nd harmonic content for the CMUT devices is significant and much lower for the PZT-PMUT devices.

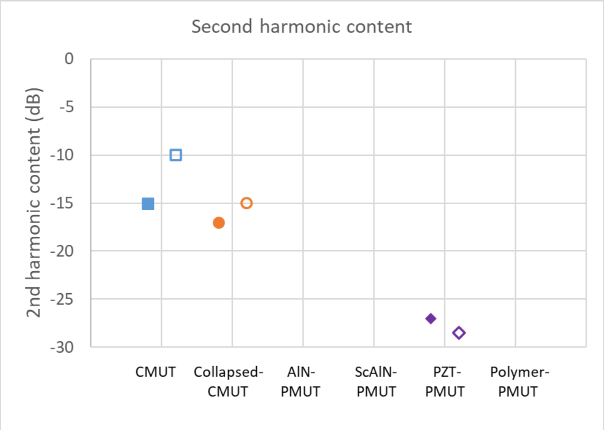

*Figure 31 First over second harmonic content (dB at 0.7MPa output pressure). For each MUT technology, the LF devices are marked with filled markers (e.g. •) and the HF devices are marked with open markers (e.g. **o**).*

The accuracy of the 2nd harmonic content is limited, especially for the lower levels. For the measurements, a rectangular driving pulse was used. Such a rectangular driving pulse contains higher harmonics in the range of -35 to -17 dB, depending on the test device. An interaction between the pulse shape and the device under test was observed. This means that the outcome for the PZT-PMUT devices is probably dominated by these issues; the real values may even be better than the values shown in Figure 31.

Strategies to reduce harmonic distortion include optimizing the device design for maximal output on the first harmonic and the use of pre-distorted excitation (at the cost of efficiency).

5.2 Link between technology and clinical application

In this part, we will discuss the link between the benchmark results and the potentials of the different MUT technologies for various clinical applications.

5.2.1 Clinical application aspects

Application space
From the application space presented in Table 5, it appears that the low-frequency range covers several core applications: echocardiography, obstetric imaging, general abdominal imaging, and others.

Acoustical aspects
Table 6 summarizes the clinical impact of the acoustical benchmark parameters for ultrasound imaging.

For ablation, a transurethral HIFU application is used as a reference. For such an application a good acoustical intensity, steering accuracy and resolution are key. Linearity and harmonic distortion are important for a well-controlled ablation. For the benchmark, the most impactful parameters are maximal peak-to-peak pressure and transmit sensitivity.

For wearables, the reference is a comfortable patch that contains one or more US modules for monitoring and diagnostic. The clinical requirements are considered similar to low-end imaging. So similar to Table 6, with more focus on power consumption, electrical safety and integration, and more relaxed on image resolution (BW), frame rate, penetration depth (peak-to-peak pressure) and harmonic imaging.

Table 5 Application space.

	Clinical Application	Frequency Range
Cardiovascular	Echocardiography Transoesophageal Echocardiography Intracardiac Echocardiography (ICE)	1.5 - 4.5 MHz 3 - 7 MHz 3 - 20 MHz
General imaging	Abdominal Vascular Musculoskeletal	3 - 7 MHz 5 - 10 MHz 8 - 20 MHz
Women's health	Obstetrics and gynecology Breast	3 -10 MHz 5 - 10 MHz
Intravascular	Intravascular Ultrasound (IVUS) Doppler guide wire	>20 MHz >20 MHz
Therapy	Ablation (HIFU)	3 - 5 MHz
Wearables	Monitoring and diagnostics	1-10 MHz

Table 6 Clinical impact of the acoustical benchmark parameters for ultrasound imaging.

Measured parameter	Clinical impact	Requirement
Max peak-to-peak pressure	• Penetration depth, harmonic imaging • Trade-off with lifetime	• As high as possible. • > 1 MPa (at surface) for harmonic imaging
Transmit sensitivity	• No direct clinical impact. • Relates to device efficiency and RF voltage needed	As high as possible.
Receive sensitivity	• Dynamic range, contrast resolution, penetration depth	As high as possible
Center frequency	• Is a design parameter • Penetration depth, axial resolution, radial resolution	
Fractional bandwidth	• Axial resolution (pulse length), sensitivity for 2nd harmonic, frequency tuning	As high as possible
Linearity	• Non-linear behavior complicates signal processing and limits the use for certain applications	As linear as possible.
Harmonic distortion	• Harmonic imaging mode is very important for echocardiography. Also important for the contrast-enhanced ultrasound that exploits the nonlinear scattering characteristics of microbubbles	As low as possible.

System aspects

The parameters measured in the air-coupled impedance measurements are most relevant for the system aspects. The obtained impedance and resistance values can impact the efficiency of the signal chain. High impedance and series resistances can result in slower switching times, larger currents, heat generation and reduced signal-to-noise ratio.

Heat generation can be an integration issue. Electronics can be adapted to match the thermal requirements, but this comes at the costs of reduced imaging performance (reduced frame rate, using limited elements, restrictions on imaging modes).

A high DC bias voltage gives none or only limited complications for integration with an ASIC. The ASIC is typically electrically decoupled from the bias voltage (DC isolated via a capacitor) and electrically floating at a high voltage and isolated with a dielectric material from the environment.

A suitable ASIC technology is to be selected that fits the needed RF switching voltage levels. Switching voltage levels up to 70-200V are fairly common, where SOI technology allows for higher voltages. In general, it is beneficial to have a lower RF voltage. A HV technology has certain disadvantages. HV technologies need larger devices (more real estate on the chip) and results in a compromised performance (slower switching, charge injections, parasitic transmissions). This can result e.g. in limitations for the ultrasound element pitch, especially for integration with 2D matrix arrays. This is less critical for linear transducers and for transducers where the front-end electronics are not integrated within the probe.

Electrical safety aspects

Electrical safety is most relevant for wearables and in-body devices, especially for catheters with their dimensional constraints.

The switching RF voltage itself is not considered a safety risk.

There are different high DC voltage lines, depending on the need for a DC bias.

- DC bias voltage level is a risk. A DC bias line is not supplying electrical power so safety can be de-risked by adding a current protection circuit. The current protection depends a.o. on the amount of charge stored (capacitance) and can be as simple as a high series resistance.
- There is always a DC power supply to the chip that generates the HV switching waveforms. This DC supply line is to deliver power and cannot be protected by high series resistance. The electrical safety of this high voltage line is to be guaranteed via other solutions, e.g. via dielectric protection.

5.2.2 Benchmark results and clinical applications

In this part, we will discuss the outcomes of the benchmark in relation to the selected clinical applications.

An overview of the benchmark results in relation to the clinical applications is summarized in Table 7 below.

Table 7 Outcomes of the benchmark.

	Strong	Limitations
CMUT	• Maturity sufficient for most medical applications • Combination of good peak-to-peak pressure, transmit pressure sensitivity and highest receive sensitivity makes this technology promising for medical imaging and ablation • High BW due to membrane design freedom for high axial resolution and frequency range • No Pb for disposables	• 2nd Harmonic content may need to be improved for echocardiography and ICE • Some devices show linearity issues which may limit certain applications • High DC operation voltage complicates catheter-based imaging and wearables
Collapsed-CMUT	• Maturity sufficient for most medical applications • Combination of good peak-tp-peak pressure, highest transmit pressure and high receive sensitivity make this technology promising for medical imaging and ablation • No Pb for disposables	• 2nd Harmonic content may need to be improved for echocardiography and ICE • High DC operation voltage complicates catheter-based imaging and wearables
AlN-based PMUT	• No DC bias voltage beneficial for in-body applications and wearables • No Pb for disposables	• Technology to be matured
PZT-PMUT	• High output pressure and very low second harmonic content make this technology a promising candidate for imaging and ablation • Low DC bias beneficial for in-body applications and wearables	• Technology to be matured • Intrinsic large capacitance related to a high dielectric constant of PZT reduces receive sensitivity
Polymer PMUT	• No Pb for disposables	• Technology to be matured • Medical imaging may not be the most obvious application

6 Conclusions and recommendations

Europe is at the forefront of the development of MEMS ultrasound transducers. In this white paper, the results of a unique pan-European benchmark of MUT technologies are summarized. CEA Leti, Fraunhofer IPMS, Imec, Kessler Foundation for Research (FBK), Philips, Roma Tre University, Silex Microsystems AB, Vermon and VTT Technical Research Centre of Finland with their CMUT and PMUT technologies participated in this benchmark.

All the participating partners have provided test dies that fulfill the pre-defined device specifications. Furthermore, all the available technologies have been characterized using the same air-coupled impedance and acoustic test protocols and set-ups. From the obtained measurement results, relevant performance parameters have been extracted and they provided the following insights on the characterized CMUT and PMUT technologies:

- There is a difference in the maturity level of CMUT and PMUT technologies and CMUT technologies are more mature at this moment;
- The most mature conventional and collapsed CMUTs show the best overall acoustical performance and they demonstrate comparable round-trip sensitivity.
- CMUT technologies demonstrate a higher bandwidth;
- PZT PMUTs show a maximum transmit pressure that is comparable to collapsed CMUTs. Furthermore, this technology demonstrates the best linearity and the lowest harmonic distortion level;
- PMUTs require no (ScAlN and AlN PMUT) or a very low operational bias voltage (polymer and PZT PMUT).

The best-performing CMUTs from this benchmarking are at a level close to the performance characteristics of the conventional poly-crystalline piezoelectric transducers, because of their maximum output pressure, receive sensitivity, and very high bandwidth. Therefore, they can be used in most clinical applications. The most benefit from using CMUTs is in high volume, high-frequency medical applications. High frequency and high bandwidth result in a high imaging resolution. PZT PMUTs show the potential to be used for therapeutic applications. If this technology is further matured and receive sensitivity is optimized, it has the potential to cover a wider range of diagnostic applications. ScAlN and AlN PMUTs contain no lead, use no DC bias and these features are very attractive for (disposable) implantable and patch applications. With ScAlN PMUTs it is possible to achieve higher coupling coefficients than AlN PMUTs, and therefore if the process flow and the orientation of the polycrystalline material are further improved, ScAlN may become very attractive for these medical applications. Other PMUT technologies need to be further matured in order to be used for ultrasound imaging or treatment applications.

While the acoustic test set-ups, test protocols, and the extraction of related performance parameters were done according to the relevant standards [refs 11,9], no standards exist describing how air-coupled impedance measurements should be done on MEMS ultrasound transducers. It can be very beneficial to introduce a standard that describes how to perform air-coupled impedance measurements on MEMS technologies and which parameters to extract. Furthermore, a critical parameter specification can be proposed that describes a good quality MEMS device. This can be very useful for the quality control of MEMS ultrasound devices.

The measurements in the laboratories at Philips were initially planned to be performed in the presence of the respective partner. Due to the pandemic of the Corona-19 virus, all the measurements were performed having the partners remotely available (via e-mail, telephone, or other communication means) during the measurements. This created additional challenges especially when an unexpected device behavior happened. Having the MEMS technology expert available in the lab during the device characterization significantly speeds up the measurement process.

From this benchmark the following aspects can be improved in order to further increase the quality of such a benchmark:

- In the benchmark, we have decided to use the same transmit and receive electronics for all acoustic measurements and all CMUT and PMUT technologies. The driving electronics have been designed with the experts that had the most knowledge on CMUTs. PZT PMUTs have a large capacitance and that somewhat impacted the results. Therefore, the driving electronics and the aperture size of the test devices may be additionally optimized for PZT PMUTs.
- Measurements should also be performed on multiple devices and statistical analysis of the obtained measurement data can be done as described in [refs 11, 16].
- Other measurement protocols such as angular directivity, impedance measurement in water, lifetime measurement of the benchmark devices will provide additional insights on the device and technology performance.

Despite all these future improvement points, the results presented in this report very well represent the status of the devices that have been characterized.

Outlook

CMUT and PMUT devices have their characteristics and strengths and will co-exist. Both technologies use semiconductor fabrication technologies and enable miniaturization, integration and high volume production at low-cost levels.
CMUTs are more suitable for medical imaging. Their high operation frequency and acoustic performance results in better image quality. Their high sensitivity makes CMUT also a very sensitive sensor with high-temperature stability (up to 200 – 500°C). Potential applications include e.g. chemical, biological sensing, and engine oil sensors.
PZT PMUTs can be used for therapeutic applications and shows the potential to cover a wider range of diagnostic applications. Furthermore, PMUTs could be used for air-coupled applications in consumer or automotive sensing applications (e.g. obstacle detection, gesture recognition, gaming, fingerprint sensor) and actuators. The main strength of AlN-based PMUTs is that no DC-bias voltage is needed. This is interesting for low power applications (e.g wearables like bladder level monitoring, blood pressure monitoring, cardiac monitoring) and USB-powered devices.
Potential applications for polymer PMUTs are implantables, health-related consumer applications (wearables), air-coupled applications, embedded in displays (haptics), acoustic interfacing, applications that can use flexibility and transparency.

7 Acknowledgements

The following persons contributed to the writing and compilation of this whitepaper:

Cees Visser
Philips Research
c.g.visser@philips.com

Alessandro Savoia
Roma Tre University
alessandro.savoia@uniroma3.it

Nenad Mihajlovic
Philips Research
nenad.mihajlovic@philips.com

Rob van Schaijk
Philips Engineering Solutions
rob.van.schaijk@philips.com

Peter Loebl
Philips Research
peter.loebl@philips.com

Marco Kircher
Fraunhofer Institute for Photonic Microsystems
marco.kircher@ipms.fraunhofer.de

Cyril Karuthedtah
VTT Technical Research Centre of Finland
cyril.karuthedath@vtt.fi

Peter Ågren
Silex Microsystems AB
peter.agren@silex.se

Guilherme Brondani Torri
Imec
Guilherme.BrondaniTorri@imec.be

Alvise Bagolini
Kessler Foundation for Research (FBK)
bagolini@fbk.eu

Dominique Gross
Vermon
d.gross@vermon.com

Bruno Fain
CEA Leti
bruno.fain@cea.fr

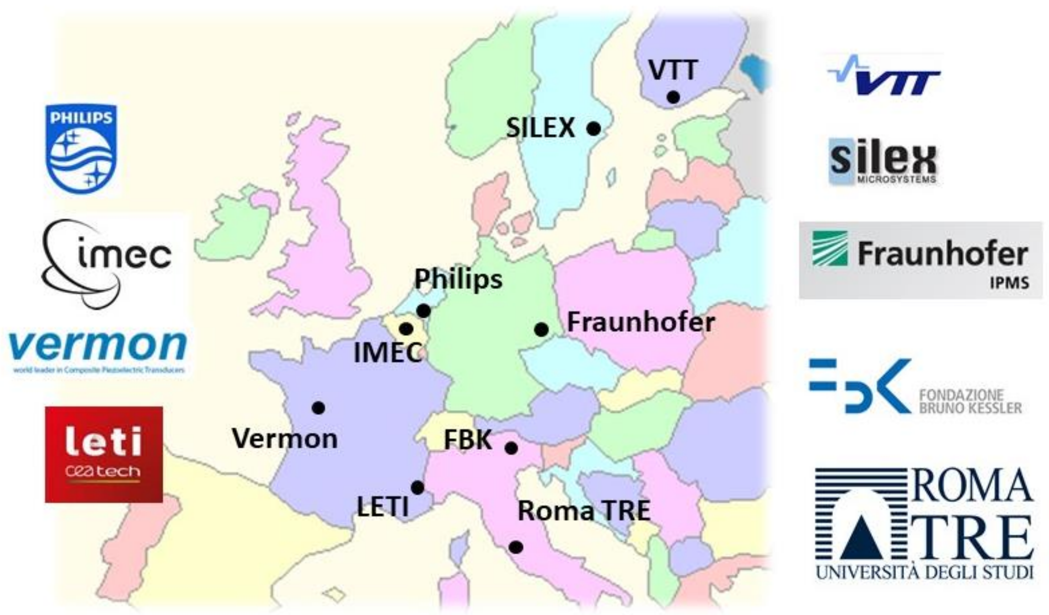

8 Abbreviations

ALD	Atomic layer deposition
AlN	Aluminum Nitride
ASIC	Application-specific integrated circuit
BAW	Bulk acoustic wave
CMOS	Complementary metal oxide semiconductor
DC	Direct current
EM	Electromechanical
HF	High frequency
ICE	Intracardiac echocardiography
IVUS	Intravascular ultrasound
CMUT	Capacitive micromachined ultrasonic transducer
DRIE	Deep reactive-ion etching
EM	Electromagnetic
FEOL	Front-end-of-line
FF	Far field
HIFU	High intensity focussed ultrasound
HV	High voltage
ICT	Information communication technology
LF	Low frequency
MEMS	Micro-electromechanical systems
MUT	Micromachined ultrasonic transducer
NEMS	Nano-electromechanical systems
NF	Near field
OLED	Organic light-emitting diode
Pb	Lead
PMUT	Piezoelectric micromachined ultrasonic transducer
P(VDF-TrFE)	Polyvinylidene Fluoride-trifluoroethylene
PVDF	Polyvinylidene flouride
PZT	Lead zirconate titanate
RF	Radio frequency
RTO	Research and technology organization
R&D	Research and development
SAW	Surface acoustic wave
ScAlN	Scandium doped Aluminium Nitride
Si	Silicon
SOI / C-SOI	Silicon on insulator / cavity silicon on insulator
TEE	Transesophageal echocardiography
TSV	Through-silicon via
US	Ultrasound

.

9 Appendix: Partners and device fabrication approaches

CEA Leti

CEA is a French government-funded technological research organization. Although public, CEA-Leti gets most of its funding from cooperative projects such as POSITION II, bilateral projects with industrials or from licensing its patent portfolio. Drawing on its excellence in fundamental research, CEA activities cover three main areas: Energy, Information and Health Technologies, and Defense and Security. The CEA-Leti excels in micro and nanotechnologies and their applications, from photonics to wireless devices, to systems for biology and healthcare.

Microsystems (MEMS) are at the core of their silicon activities. The CEA-Leti has been working on MEMS components since 1978. It has developed many microsystems components including mechanical sensors and actuators, optical and magnetic sensors and micromachined ultrasonic transducers. With a total workforce on MEMS activities of 200 permanent researchers, completed by PhD students, CEA-Leti is today one of the biggest actors in the world in this particular field. As the main driver of the MINATEC innovation campus, CEA-Leti operates 8,000-m² of state-of-the-art clean rooms in 24/7 mode, on industry-standard 200mm and 300mm wafer sizes. Strongly committed to the creation of value for the industry, CEA-Leti puts a strong emphasis on intellectual property and owns more than 300 patents in this particular field.

In the POSITION-II project, CEA Leti proposes three types of devices: low-frequency and high-frequency CMUT devices, as well as high-frequency PMUT devices based on AlN technology. CEA Leti develops CMUTs and PMUTs for airborne and water-coupled applications for low (50 – 500 kHz) and high frequencies (MHz range). In the POSITION-II project, low and high-frequency CMUT devices and high-frequency PMUTs suitable for catheter applications are utilized.

Fraunhofer Institute for Photonic Microsystems

Fraunhofer IPMS is a worldwide leader in research and development services for electronic and photonic microsystems in the fields of Medical & Health applications, Smart Industrial Solutions, and Improved Quality of Life. Innovative products can be found in all large markets – such as ICT, consumer products, automobile technology, semiconductor technology, measurement and medical technology-based upon various technologies (e.g. MEMS micro mirrors, micro gratings, micro mirror arrays, chemical sensor, and ultrasound and acoustics sensor) developed at Fraunhofer IPMS.

In the MEMS ultrasound field, Fraunhofer IPMS provides the complete value-added chain from R&D to pilot fabrication comprising consulting, design, prototyping, characterization, electronics, data processing and pilot fabrication based on different MUT technologies in its 200mm state-of-the-art clean room. Highly reproducible CMUT arrays are available for airborne and liquid-coupled applications such as flow metering, Doppler-ultrasound, surface and volume imaging. The unique selling point of Fraunhofer IPMS' air-coupled CMUTs is their high transmit and receive frequencies of 1-5MHz. This allows unprecedented resolutions at minimum distances to the sensor, which opens up new areas of application. CMUT development kits with associated sensor solutions are provided by Fraunhofer IPMS to lower the obstacles for customers regarding their ultrasound developments based on CMUTs. Within this benchmark, Fraunhofer IPMS participated with non-collapse CMUTs for the low-frequency and high-frequency target specifications. The device frequencies produced for the benchmark represent only a portion of the available range for tissue-coupled CMUTs.

Imec

Imec is a world-leading R&D and innovation hub in nanoelectronics and digital technologies. It leverages its scientific knowledge and delivers industry-relevant technology solutions with the innovative power of its global partnerships in ICT, healthcare, and energy. In a unique high-tech environment, its international top talent is committed to providing the building blocks for a better life in a sustainable society. Imec is headquartered in Leuven, Belgium, and has offices also in the Netherlands (so-called Holst Centre in collaboration with TNO), Taiwan, USA, China, India and Japan.

At its Headquarters in Leuven, Imec has two clean rooms that run a semi-industrial operation (24/7, all year round). The 300mm pilot line, used for R&D on (sub-)22nm process technology. In the 200mm cleanroom, heterogeneous integration is being explored which supports manufacturing with added functionality, such as sensors, actuators, MEMS and NEMS. Finally, within the Smart System activities, a large group of Imec has world-renown expertise in flexible electronics and related applications, in particular medical sensing arrays and OLED displays.

Imec offers three business models: (1) Development-on-demand (design and prototype fabrication) of ultrasound transducer array devices for specific application purposes (relevant for medical device companies but also clinical partners). (2) Further technology upscaling and low-volume production for development-on-demand partners to bridge the prototype-to-volume production gap (relevant for medical device companies). (3) Technology licensing and transfer to foundries and fabrication partners (important to support large volume production, either supporting medical device companies that do not want to own fabrication or to allow widespread use of the MUT platform technology for companies that also have their design capabilities).

Imec has significant expertise in developing MEMS ultrasound transducer technology platforms for water- and air-coupled devices. Imec expertise spans from device design and simulation to process development and fabrication. In the POSITION-II MEMS ultrasound transducer benchmark, Imec explored two PMUT technologies.

The first technology is built on large-area polymer-based flexible substrates with piezoelectric materials such as PVDF. With the Imec polymer-based PMUT technology large and flexible arrays can be produced. This might enable novel applications in the medical and consumer markets, ranging from catheters to wearable and disposable devices. Fabrication is compatible with existing display technologies, which lowers the costs and eases the integration with drive and sense electronics. Flexible substrates facilitate the integration of ultrasound arrays into medical catheters. This technology is undergoing rapid development with research in new materials and process flows focusing on further increasing performance.

The second technology is based on conventional silicon wafers using PZT as piezoelectric material. For the POSITION-II project, Imec developed a new process flow to produce PZT-PMUT transducers. The fabrication starts with an SOI or C-SOI wafer where the PZT stack is deposited by ALD. The cavities are formed by DRIE. The process flow has been set-up and lots have been processed part in the lab-environment and part in the pilot-line. Process modules have been successfully demonstrated, but due to time constraints, the device lots were not ready on time for the benchmark measurements.

Philips

Philips is a leader in health technology. At Philips, our purpose is to improve people's health and well-being through meaningful innovation. Guided by this purpose, it is our strategy to lead with innovative solutions that combine systems, smart devices, informatics and services, and leverage big data

Our Research activities help shape the future by exploring how to best apply advances in science and technology to create impactful innovations, often in partnership with the broader innovation community. One of the key areas of expertise is to design, develop and manufacture custom MEMS and assemble micro devices at our MEMS Foundry and Micro Devices Facility. The Philips MEMS Foundry is a pure-play foundry delivering micro-fabricated devices for both Philips as well as external customers. One of our important technology platforms is based on CMUTs. This technology is well suited and optimized for medical applications, ranging from general probes towards integration in catheters. For the first applications, it leverages the main CMUT advantages of high volume manufacturing, low cost and high performance leading towards ubiquitous ultrasound. Our CMUT devices use the so-called collapse mode, with cells designed such that part of the (electrically isolated) membrane is in physical contact with the substrate during normal operation. Our collapse mode designs enhance the transmit and receive sensitivities (ref 17). For catheter-based devices, CMUT technology also adds high levels of integration and miniaturization.

Roma Tre University

Founded in 1992, Roma Tre University is an Italian public research university located in Rome, Italy. Organized in 2 schools and 12 departments, Roma Tre offers 54 undergraduate degree programs, 75 master's degree programs, and 23 Ph.D. programs, and currently enrolls more than 35 thousand students. It is the second-largest university of Rome by enrollment and one of the largest research-based institutions in the country.

The Department of Engineering of Roma Tre University currently hosts 110 professors and conducts international research in the fields of electronics and biomedical engineering, computer science, mechanics, and civil engineering.

The Acustoelectronics Laboratory (ACULAB) of the Department of Engineering was founded in 1996. Its core research focuses on CMUT and PMUT for medical imaging applications and includes transducer modeling and design, microfabrication technologies, packaging, characterization, and system integration. As the first university laboratory in the world to demonstrate in vivo ultrasound imaging with CMUT probes in 2003, ACULAB has developed several CMUT and PMUT-based 1D and 2D ultrasound probes operating in a wide frequency range (2-18 MHz) for different medical imaging applications. Its facilities include a computer room equipped with software tools developed for ultrasonic transducer design, a cleanroom dedicated to acoustic material processing and transducer packaging, and a laboratory for electrical and acoustic characterization and ultrasound imaging testing. ACULAB's main MEMS fabrication partner is Kessler Foundation for Research (FBK).

Kessler Foundation for Research (FBK)

FBK is the top research institute in Italy, ranked in the first place for scientific excellence within three different subject areas and the economic and social impact according to the latest quality of research ANVUR evaluation.

With its 3,500 square meters of laboratories and scientific infrastructures and a community of over 400 researchers, 140 doctoral students, 200 visiting fellows and thesis students, 700 affiliates and accredited students combined, FBK acts as a scientific and technological hub, its premises and platforms hosting a lively ecosystem of co-located ventures, spin-offs, projects and training opportunities.

The result of more than half a century of history, through 11 centers dedicated to technology and innovation and the humanities and social sciences, FBK aims to achieve excellent results in the scientific and technological field with particular regard to interdisciplinary approaches and the application dimension.

This is due to the constant focus on collaborations and exchange activities with public administration and institutions, small, medium-sized and multinational companies, European and international institutions, which broaden the capacity for innovation and involve the local community and the local economy in the circulation of knowledge and technologies. The Sensors and Devices Center focuses on highly integrated sensors and devices, products of excellence in research and industrial innovation, based on

MEMS, CMOS, photonics and surface functionalization techniques and interfaces.

Silex Microsystems AB
Silex Microsystems, the world's largest pure-play MEMS foundry, is driving the sensory system revolution, partnering with the world's most innovative companies to commercialize MEMS technologies. Silex offers the industry's most advanced MEMS and heterogeneous wafer-level packaging and state-of-the-art MEMS manufacturing tools & equipment with production operations totaling 25,000 square feet, giving customers a strategic path to high volume. Our standard processes include proven technologies and proprietary processes such as the Silex Sil-Via® TSV and Zero-Crosstalk™ isolating substrate. Incorporating state-of-the-art deposition, etching and electroplating equipment in our 8-inch fab enables us to offer unique functional capping technologies with integrated through-wafer metal vias, RF passives and coaxial feedthroughs. We also have a fully equipped PZT production line with superior PZT performance.
Our customized software for product development and production control allows us to manage a widely diverse product and process mix, while guaranteeing consistency in process control and quality. Our system allows for the intelligent reuse of common process steps which allow for rapid prototyping and customization while maintaining processing consistency.

Vermon
Vermon SA, created in 1984 is one of the world's leading companies in ultrasound transducers for imaging applications. The company was a spin-off from the University of Tours (France). Since the beginning, Vermon is continuously maintaining its commitment to research and technological development in the domains of ultrasonic apparatus and medical diagnosis and therapy and devotes yearly more than 20% of its revenue to R&D activities. As a result, the company owns dozens of patented technologies relating to transducers and ultrasonic medical devices and is ranked as one of the most important medical ultrasonic device manufacturers around the world. The product range covers multi-channel array transducers, 2D-matrix arrays, IntraCardiac Echography (ICE) catheters and 4D imaging probes dedicated to real-time volume rendering that make Vermon the most important and reliable supply source for Ultrasound in Europe. Transducer technologies are part of Vermon's core business and the company also develops proprietary technologies and customized solutions such as piezo composite wherein flexibility and adaptability are superior to conventional devices or capacitive Micromachined Ultrasonic Transducers (CMUTs) using MEMS technologies for performance enhanced devices for therapy and imaging. Innovation is the company's leitmotiv and Vermon is sustainably supporting collaborative research programs to develop new technologies and processes in order to maintain its competitiveness at the European level.

VTT Technical Research Centre of Finland Ltd
VTT Technical Research Centre of Finland Ltd is a state-owned and controlled non-profit limited liability company established by law and operating under the ownership steering of the Finnish Ministry of Employment and the Economy. VTT is an RTO whose activities are focused on three areas: carbon neutral solutions, sustainable products and materials, and digital technologies. VTT can combine different technologies, produce information, upgrade technology knowledge, and create business intelligence and value-added for its stakeholders. We go beyond the obvious to help society and companies to grow through technological innovations.
Microelectronics is one of the main fields of our research. VTT helps to design, develop and manufacture innovative new semiconductor components for a wide range of

applications. With decades of experience in microfabrication, we have developed multiple technology platforms, which can be used to quickly and cost-effectively develop new components. We have vast experience in international, national and industrial research projects where microfabrication has been successfully utilized for the development of novel MEMS components such as Gyroscope, Accelerometers, Micromirrors, Resonators, Pressure sensors, PMUTs/CMUTs, Acoustic emission sensors, BAW/SAW filters, etc.

VTT has strong expertise in the development of the PMUT component and PMUT enabled systems. We have capabilities to design, fabricate and characterize air and water-coupled PMUTs. Our PMUT technology is based on an in-house developed CMOS compatible AlN and ScAlN piezo MEMS platform. We have developed various processes for fabricating PMUTs. The backside DRIE release-based PMUT process is a Si wafer-based 6 mask process. This is suitable for fabricating very cheap air-coupled PMUTs of resonance frequency in the range of 100 kHz to 1.5 MHz. Cavity SOI (C-SOI) based PMUT processes are capable of fabricating water-coupled PMUT arrays with center frequencies from 1 MHz to 25 MHz. This process is very simple and requires only 5 masks. Our sacrificial layer-based process is capable of fabricating high-density vacuum cavities in a Si wafer. This process is suitable for fabricating very high-frequency water-coupled PMUTs (up to 50 MHz).

10 References

[1] www.position-2.eu

[2] A.S. Savoia (Roma Tre University), private communication

[3] www.usa.philips.com/healthcare/product/HC989605409281/x6-1

[4] Rob van Schaijk, CMUT: A Versatile Ultrasonic Platform Developed by Philips, *MEMS Seminar* 2019.

[5] K. Brenner et.al., Advances in Capacitive Micromachined Ultrasonic Transducers, *Micromachines* 10 (2), 2019, 152.

[6] Haleh Nazemi et.al., Mass Sensors Based on Capacitive and Piezoelectric Micromachined Ultrasonic Transducers – CMUT and PMUT, *Sensors* 2020, 20 (2010), 1-17.

[7] P. Gijsenbergh, A. Halback, Y. Jeong, G. B. Torri, M. Billen, L. Demi, C. H. Huang, D. Cheyns, X Rottenberg, V. Rochus, Characterization of polymer-based piezoelectric micromachined ultrasound transducers for short-range gesture recognition applications, *Journal of Micromechanics and Microengineering*, vol. 29, no. 7, p. 074001, Jul. 2019, doi: 10.1088/1361-6439/ab1f41.

[8] R. Beck, U. Pittermann, K. G. Weil, Impedance Analysis of Quartz Oscillators, Contacted on One Side With a Liquid, *Berichte der Bunsengesellschaft für physikalische Chemie*, 92, pp. 1363 – 1368, 1988.

[9] R. N. Thurston, W. P. Mason, *Physical acoustics: principles and methods*. New York, Academic Press, 1964.

[10] G. G. Yaralioglu, A. S. Ergun, B. Bayram, E. Haeggström, and B. T. Khuri-Yakub, Calculation and measurement of electromechanical coupling coefficient of capacitive micromachined ultrasonic transducers, *IEEE Trans. Ultrason. Ferroelectr. Freq. Control*, vol. 50, no. 4, pp. 449–456, Apr. 2003.

[11] International Electrotechnical Commission, IEC 62127-1 ed 1.1, *Measurement and characterization of medical ultrasonic fields up to 40 MHz*, Geneva, IEC, 2013.

[12] International Electrotechnical Commission, IEC 60854 TR ed 1.0, *Methods of measuring the performance of ultrasonic pulse-echo diagnostic equipment*, Geneva, IEC, 1986.

[13] Precision Acoustics, *Technical Data Sheet 0.2 mm Needle Hydrophone*.

[14] E. F. Arkan and F. L. Degertekin, Analysis and Design of High-Frequency 1-D CMUT Imaging Arrays in Noncollapsed Mode, *IEEE Transactions on Ultrasonics, Ferroelectrics, and Frequency Control*, vol. 66, no. 2, pp. 382-393, Feb. 2019, doi: 10.1109/TUFFC.2018.2887043.

[15] O. Oralkan, S. T. Hansen, B. Bayram, G. G. Yaralioglu, A. S. Ergun and B. T. Khuri-Yakub, High-frequency CMUT arrays for high-resolution medical imaging, *IEEE Ultrasonics Symposium*, 2004, Montreal, QC, Canada, 2004, pp. 399-402 Vol.1

[16] International Organization for Standardization, ISO 16269-6:2005, *Statistical interpretation of data – Part 6: Determination of statistical tolerance intervals*, Geneva, ISO, 2005.

[17] R.P. Zangabad et al., Real-Time Coded Excitation Imaging Using a CMUT-based Side Looking Array for Intravascular Ultrasound, *IEEE Transactions on Ultrasonics, Ferroelectrics, and Frequency Control*, Vol. 68, No. 6, June 2021, 2048-2058.